Published in final edited form as:
Science. 2012 June 22; 336 (6088):1585-1588. doi: 10.1126/science.1220111

The Fission Yeast FANCM Ortholog Directs Non-Crossover Recombination During Meiosis

Alexander Lorenz, Fekret Osman, Weili Sun, Saikat Nandi, Roland Steinacher, Matthew C. Whitby*

Department of Biochemistry, University of Oxford, South Parks Road, Oxford OX1 3QU, UK

The formation of healthy gametes depends on programmed DNA double strand breaks (DSBs), which are each repaired as a crossover (CO) or non-crossover (NCO) from a homologous template. Although most of these DSBs are repaired without giving COs, little is known about the genetic requirements of NCO-specific recombination. We show that Fml1, the Fanconi anemia complementation group M (FANCM)-ortholog of *Schizosaccharomyces pombe*, directs the formation of NCOs during meiosis in competition with the Mus81-dependent pro-CO pathway. We also define the Rad51/Dmc1-mediator Swi5-Sfr1 as a major determinant in biasing the recombination process in favour of Mus81, to ensure the appropriate amount of COs to guide meiotic chromosome segregation. The conservation of these proteins from yeast to Humans suggests that this interplay may be a general feature of meiotic recombination.

*To whom correspondence should be addessed. E-mail: matthew.whitby@bioch.ox.ac.uk
Key words: Homologous recombination; Meiosis; Fml1; Mus81; *Schizosaccharomyces pombe*

Faithful chromosome segregation during meiosis depends on the establishment of chiasmata through recombinational repair of programmed DNA double-strand breaks (DSBs) to produce crossovers (COs) between homologous chromosomes (homologs). However, in most cases only a minority of the DSBs are earmarked to form COs, and therefore the majority have to be repaired by using either the homolog without CO formation or the sister chromatid (*1*).

In order to identify helicase activities involved in non-crossover (NCO)-recombination during meiosis in the fission yeast *Schizosaccharomyces pombe*, we screened for helicases potentially capable of D loop unwinding during synthesis-dependent strand annealing (SDSA), which is thought to be a major pathway of NCO recombination (*1*). To this end, we used a genetic recombination assay consisting of a meiotic recombination hotspot at the *ade6* gene and two flanking scorable markers (Fig. 1A). We hypothesized that at least one of the helicases promoting NCO recombination pathways in mitotic cells would also have a role during meiosis. From our candidate list – *fbh1*, *srs2*, *rqh1*, *fml1* and *fml2* – only the deletion of *fml1* gave the expected increase in CO formation associated with a meiotic gene conversion (GC) event at two different hotspot alleles, *ade6-M26* and *ade6-3083*, and at a non-hotspot allele *ade6-M375* (Fig. 1, B and C, and tables S1 to S3) (*2–5*). Increases in COs were also observed on a different chromosome (Fig. 1D and table S4) and by a physical assay at the *mbs1* locus (fig. S1), indicating that Fml1's role in suppressing CO formation is not restricted to a single locus.

In vitro purified Fml1, like its budding yeast ortholog Mph1, unwinds D loops and is therefore suited to promoting SDSA (Fig. 1E) (*6, 7*). The *fml1-K99R* mutant, which encodes protein that retains full DNA

binding activity but is unable to unwind D loops (Fig. 1E and fig. S2), exhibits the same hyper-CO phenotype as the null mutant indicating that Fml1's helicase function is required for NCO formation (Fig. 1C). A significant increase in CO is also observed by deleting Fml1's cofactors Mhf1 and Mhf2, whose orthologs in humans promote the DNA binding and catalytic activities of Fanconi anemia complementation group M (FANCM) (Fig. 1C and table S2) (*8, 9*).

In fission yeast the formation of CO products from joint DNA molecules depends on the endonuclease Mus81-Eme1 (*10*). The deletion of *mus81* causes joint DNA molecules to remain unresolved, which prevents chromosome segregation and results in a reduction in the viability of progeny (Fig. 2, A and B, fig. S3 and table S5) (*10-12*). The mating efficiency of *mus81*Δ *fml1*Δ double mutants is very low (table S6), preventing comprehensive genetic analysis; however, visual inspection of *mus81*Δ *fml1*Δ asci showed a higher incidence of clumped DNA masses than in *mus81*Δ single mutants, indicating an aggravation of the chromosome segregation problem (Fig. 2B and table S7). These data indicate that at best, Fml1 only poorly substitutes for the loss of the CO recombination pathway by feeding joint molecules into a NCO pathway. The meiosis-specific Rad51-paralogue Dmc1 has been shown to form D loops, which are more resistant to dismantling by DNA translocases than those formed by Rad51 (*13*); however, in fission yeast deletion of *dmc1* does not change the level of COs associated with GCs (table S2). The Rad51/Dmc1-mediator complex Swi5-Sfr1 (*14*) is required for wild-type levels of CO and its deletion ameliorates the defects seen in a *mus81*Δ mutant (Fig. 2, A, B and C) (*15*). This rescue of *mus81*Δ by *sfr1*Δ and the reduction of CO formation associated with GC in a *sfr1*Δ single mutant depend on the presence of *fml1* (Fig. 2, A, B and C). This suggests that Swi5-Sfr1 protects D loops from being unwound by Fml1 and in doing so promotes Mus81-mediated CO formation. In accordance with this, we see a reduction in Mus81 foci in *sfr1*Δ meiotic nuclei compared with wild type (fig. S4 and table S8).

Under vegetative growth conditions *mus81*Δ *fml1*Δ strains display synthetic sickness (*6*), and therefore to confirm that the phenotypes we observe during meiosis are caused by the failure to process meiotic recombination intermediates, we abrogated meiotic DSB formation by deleting *rec12* (also termed *spo11*) in *mus81*Δ *sfr1*Δ, *mus81*Δ *fml1*Δ and *mus81*Δ *fml1*Δ *sfr1*Δ strains. The spore viabilities of the mutant combinations were higher than or similar to the 12.5% expected from random segregation of three chromosome pairs (Fig. 2D). Although the spore viability in the *mus81*Δ *fml1*Δ *rec12*Δ and *mus81*Δ *fml1*Δ *sfr1*Δ *rec12*Δ crosses is not completely restored to *rec12*Δ levels, the rescue is robust enough to attribute much of the meiotic failure of these mutant combinations to a breakdown in processing meiotic recombination intermediates.

The transcription of *mus81*, *eme1*, *swi5* and *sfr1* is upregulated (by two- to sixfold) at the start of meiosis, whereas that of *fml1* is not (*16*). Therefore, we wondered whether relative changes in the amounts of these proteins could influence whether DSBs are repaired as COs or NCOs. Indeed, Fml1 over-expression in wild type reduces COs at *ade6-3083* in a dosage-dependent manner (Fig. 3A and table S9). This effect depends on Fml1's helicase activity because overexpression of Fml1-K99R or Fml1-D196N, which can bind but not unwind D-loops (Fig. 1E and fig. S2), causes a significant increase in COs akin to *fml1*Δ (Fig. 3A and table S9). Overexpression of these mutants also confers *fml1*Δ-like sensitivity to genotoxins (fig. S5). Most likely, these mutant proteins impede endogenous wild-type Fml1 and thereby generate a *fml1*Δ-like phenotype.

Further evidence that the relative amount of Fml1 and Swi5-Sfr1 is a determinant in Fml1's ability to unwind D loops in vivo comes from analyzing the effect of Fml1 overexpression in *mus81*Δ crosses. Here both the

spore viability and chromosome segregation defects of *mus81*Δ crosses are ameliorated in a helicase-dependent manner and in a similar way as deleting *sfr1*: without producing COs (Figs. 2B and 3, A and B). As in wild-type crosses, overexpression of mutant Fml1 probably impedes endogenous wild-type Fml1, worsening the already poor spore viability and chromosome segregation of a *mus81*Δ cross (Figs. 2B and 3B and table S7). The partial rescue of spore viability and chromosome segregation in *mus81*Δ crosses is specific to Fml1 because none of the other candidate DNA helicases (Rqh1, Srs2, Fbh1, and Fml2) when overexpressed could do this (table S5).

Swapping exogenous Holliday junction (HJ) resolvases, namely bacterial RusA and human GEN1, for Mus81 results in a reduction of CO associated with GC at an *ade6* hot spot from ~60% down to ~40% (*17, 18*). Our explanation was that these HJ resolvases (in contrast to Mus81-Eme1) cleave recombination intermediates in an unbiased manner producing COs and NCOs in a 1:1 ratio. We hypothesized that the remaining 20% NCO recombination events stem from SDSA (Fig. 4A). If this is true, then exchanging Mus81 for RusA or GEN1 in a *fml1*Δ background, in which SDSA is abolished, would result in 50% COs and NCOs via unbiased HJ resolution (Fig. 4A). Indeed, 50% COs is what we find when RusA or GEN1 are expressed in *mus81*Δ *fml1*Δ strains (Fig. 4B).

It is conceivable that the Fml1-dependent NCO pathway proceeds via biased HJ cleavage rather than SDSA. However, deletion of the two known junction-specific nucleases (Slx1 and the XPF ortholog Rad16), which could potentially fulfill this function, has no effect on CO formation or spore viability in a *mus81*Δ *sfr1*Δ mutant (tables S2 and S5).

Our data show that Fml1-Mhf works in parallel with Mus81-Eme1 to process meiotic joint DNA molecules, and that Fml1's ability to produce NCOs is mitigated by a relative up-regulation of a Swi5-Sfr1 and Mus81-Eme1-dependent pathway, in which Swi5-Sfr1 may stabilize Rad51/Dmc1–mediated single-end invasions so that they can be preferentially cleaved by Mus81-Eme1. Fml1 represents the only factor directly driving a meiotic NCO-specific pathway; however, other DNA helicases, such as RTEL-1 in *C. elegans*, apparently can direct the recombination outcome via template choice, creating an additional level of regulation (*19, 20*).

References and Notes

1. M. S. McMahill, C. W. Sham, D. K. Bishop, *PLoS Biol* **5**, e299 (2007).
2. W. Sun, A. Lorenz, F. Osman, M. C. Whitby, *Nucleic Acids Res* **39**, 1718 (2011).
3. G. A. Cromie, R. W. Hyppa, G. R. Smith, *Genetics* **179**, 1157 (2008).
4. P. Schuchert, J. Kohli, *Genetics* **119**, 507 (1988).
5. W. W. Steiner, G. R. Smith, *Genetics* **169**, 1973 (2005).
6. W. Sun *et al.*, *Mol Cell* **32**, 118 (2008).
7. R. Prakash *et al.*, *Genes Dev* **23**, 67 (2009).
8. T. R. Singh *et al.*, *Mol Cell* **37**, 879 (2010).
9. Z. Yan *et al.*, *Mol Cell* **37**, 865 (2010).
10. G. A. Cromie *et al.*, *Cell* **127**, 1167 (2006).
11. M. N. Boddy *et al.*, *Cell* **107**, 537 (2001).
12. F. Osman, J. Dixon, C. L. Doe, M. C. Whitby, *Mol Cell* **12**, 761 (2003).
13. D. V. Bugreev *et al.*, *Nat Struct Mol Biol* **18**, 56 (2011).
14. N. Haruta *et al.*, *Nat Struct Mol Biol* **13**, 823 (2006).
15. C. Ellermeier, H. Schmidt, G. R. Smith, *Genetics* **168**, 1891 (2004).
16. J. Mata, R. Lyne, G. Burns, J. Bähler, *Nat Genet* **32**, 143 (2002).
17. L. J. Gaskell, F. Osman, R. J. Gilbert, M. C. Whitby, *EMBO J* **26**, 1891 (2007).
18. A. Lorenz, S. C. West, M. C. Whitby, *Nucleic Acids Res* **38**, 1866 (2010).

19. J. L. Youds *et al.*, *Science* **327**, 1254 (2010).
20. S. Rosu, D. E. Libuda, A. M. Villeneuve, *Science* **334**, 1286 (2011).
21. S. A. Sabatinos, S. L. Forsburg, *Methods Enzymol* **470**, 759 (2010).
22. G. R. Smith, *Methods Mol Biol* **557**, 65 (2009).
23. A. L. Goldstein, J. H. McCusker, *Yeast* **15**, 1541 (1999).
24. K. Maundrell, *Gene* **123**, 127 (1993).
25. A. Lorenz, F. Osman, V. Folkyte, S. Sofueva, M. C. Whitby, *Mol Cell Biol* **29**, 4742 (2009).
26. C. L. Doe, J. Dixon, F. Osman, M. C. Whitby, *EMBO J* **19**, 2751 (2000).
27. S. C. Ip *et al.*, *Nature* **456**, 357 (2008).
28. U. Rass *et al.*, *Genes Dev* **24**, 1559 (2010).
29. J. Loidl, A. Lorenz, *Methods Mol Biol* **558**, 15 (2009).
30. A. Lorenz *et al.*, *J Cell Sci* **117**, 3343 (2004).
31. R. W. Hyppa, G. R. Smith, *Methods Mol Biol* **557**, 235 (2009).
32. A. L. Grishchuk, J. Kohli, *Genetics* **165**, 1031 (2003).
33. R. W. Hyppa, G. R. Smith, *Cell* **142**, 243 (2010).
34. F. Osman, J. Dixon, A. R. Barr, M. C. Whitby, *Mol Cell Biol* **25**, 8084 (2005).
35. C. Shimoda, *J Cell Sci* **117**, 389 (2004).
36. A. Lorenz, A. Estreicher, J. Kohli, J. Loidl, *Chromosoma* **115**, 330 (2006).

Acknowledgements:
We thank R. Mercier for discussions and sharing data before publication. We are grateful to A. Decottignies, J. Kohli, R. J. McFarlane, P. Russell, G. R. Smith and W. W. Steiner for providing strains/reagents and to C. Bryer and J. Witzki for technical assistance. This work was supported by a Wellcome Trust Programme Grant 090767/Z/09/Z. A.L. was funded in part by an Erwin Schrödinger Fellowship (J 2489-B03) from the Austrian Science Fund (FWF).

Supporting Online Material:
www.sciencemag.org
Materials and Methods
Figs. S1 to S5
Tables S1 to S10
References (*21-36*)

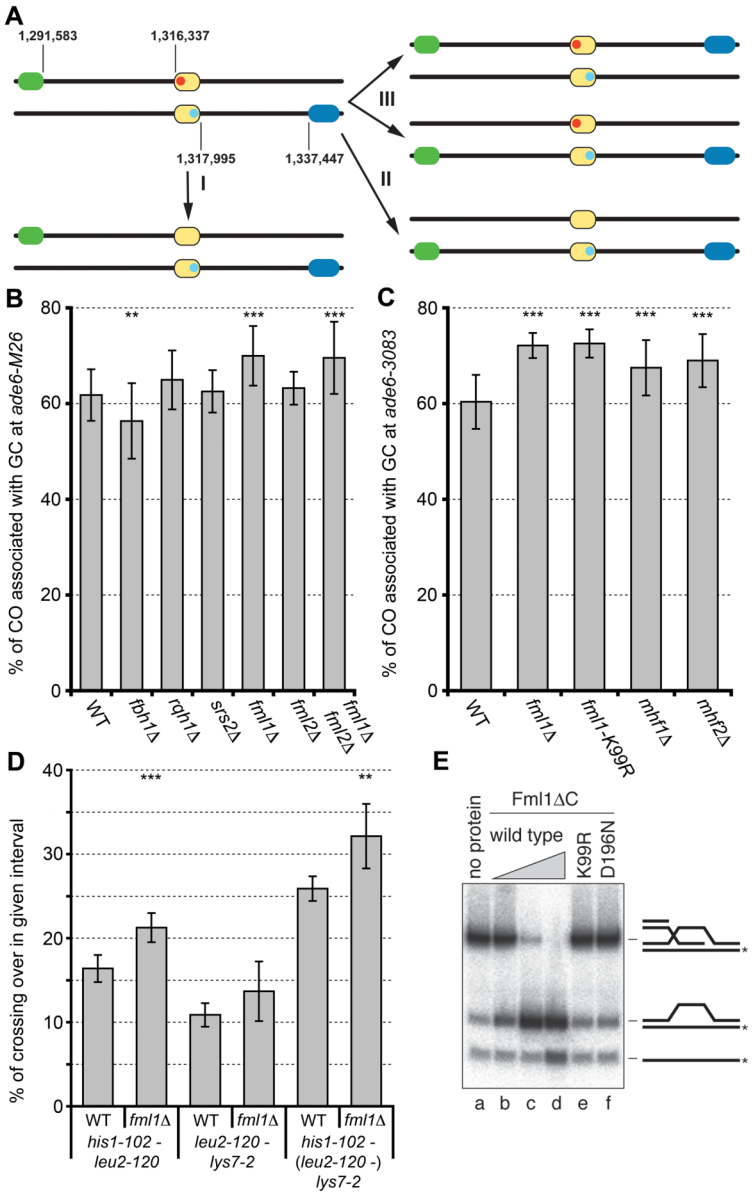

Fig. 1. Fml1-Mhf is required for wild-type levels of NCO during meiosis. (**A**) Schematic of the meiotic recombination assay indicating the positions (in base pairs) of *ura4*$^{+}$*-aim2* (green), *his3*$^{+}$*-aim* (blue) and *ade6* (yellow) on chromosome 3. The point mutations in the *ade6-3083*/*-M26* hotspot and *ade6-469* coldspot alleles are labelled in red and light blue, respectively. The common types of outcomes of the assay are shown: (I) GC at *ade6* without CO, (II) GC at *ade6* with CO of the flanking markers, and (III) CO without GC at *ade6*. (**B** and **C**) Frequency of CO associated with GC events at *ade6* hotspots in wild type and mutants (tables S1 and S2) (*2*). (**D**) Frequency of CO in two neighbouring intervals in wild type and the *fml1*Δ mutant (table S4). In (B) to (D), statistical significance in comparison with wild type indicated as **P* <0.1, ***P* <0.05, and ****P* <0.01 (for *P* values, see corresponding tables in the supplementary materials). (**E**) D loop unwinding by Fml1ΔC (lanes b to d: 0.05 nM, 0.5 nM, and 5 nM), Fml1ΔC-K99R (lane e: 5 nM) and Fml1ΔC-D196N (lane f: 5 nM). The schematics represent the D loop and its dissociation products, with the asterisk indicating the position of the 5' end ^{32}P label.

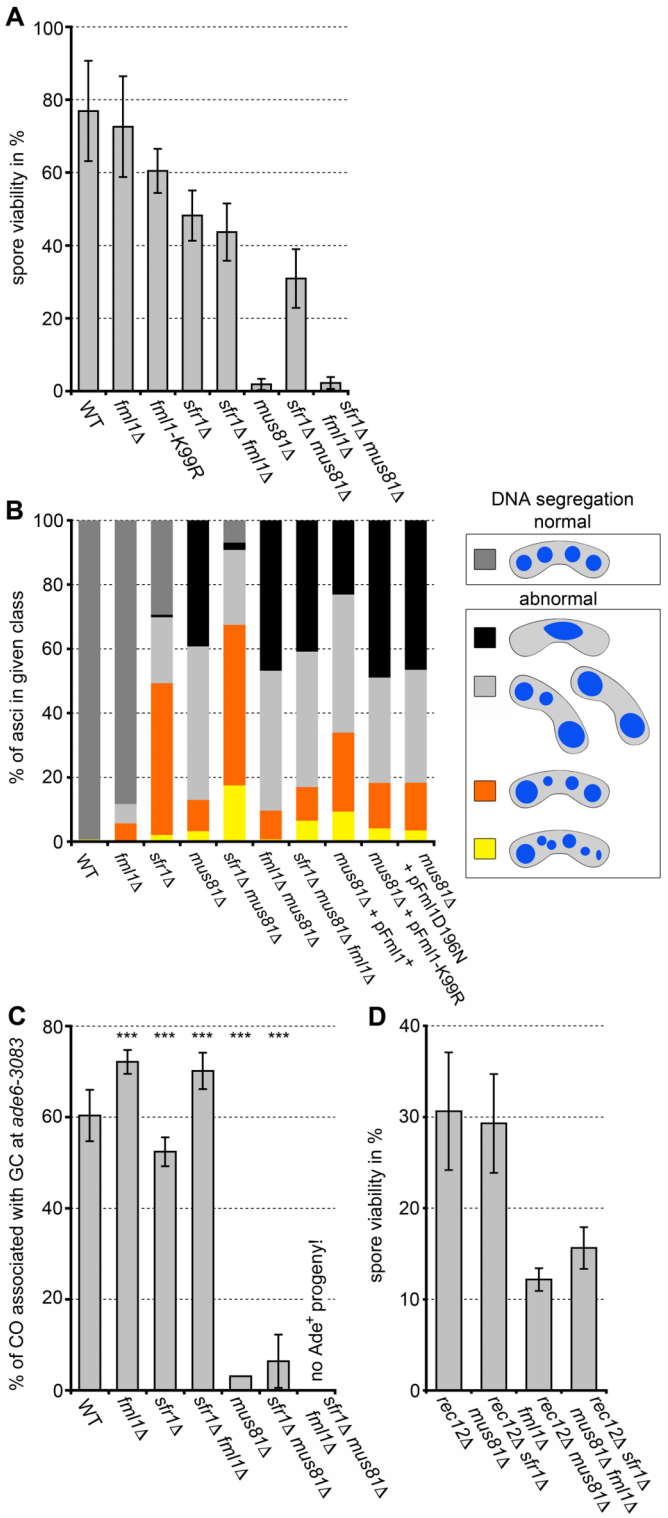

Fig. 2. Fml1 is able to drive a NCO pathway of meiotic recombination in the absence of Mus81. (**A**) Viability of progeny from wild-type and mutant crosses (table S5). (**B**) Distribution of DNA masses in wild-type and mutant asci with or without overexpression of wild-type and mutant Fml1 (fig. S3). (**C**) Frequency of CO associated with GC events at *ade6-3083* from wild-type and mutant crosses. Statistical significance in comparison with wild type is shown as **P* <0.1, ***P* <0.05, and ****P* <0.01 (table S2). (**D**) Abolishing meiotic DSB formation by deleting *rec12* partially rescues the spore viability defect of *mus81*Δ *fml1*Δ mutants (table S5).

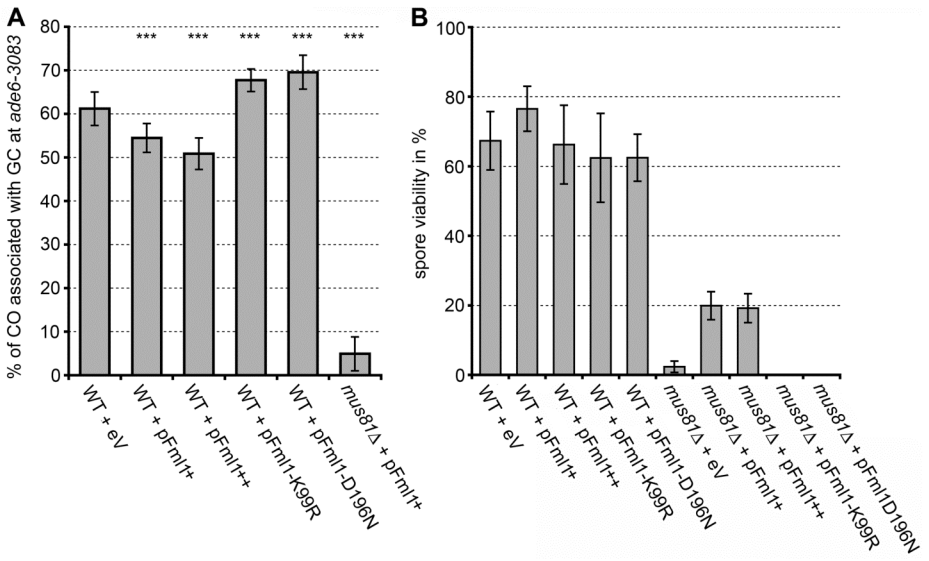

Fig. 3. Overexpression of Fml1 suppresses COs and partially rescues the poor spore viability of a *mus81*Δ mutant. (**A** and **B**) Frequency of CO associated with GC events at *ade6-3083* (A) and viability of progeny (B) in wild-type and *mus81*Δ crosses overexpressing wild-type and mutant Fml1 (tables S5 and S9). Statistical significance in comparison with wild type in (A) is shown as **P* <0.1, ***P* <0.05, and ****P* <0.01 (for exact *P* values, see table S9).

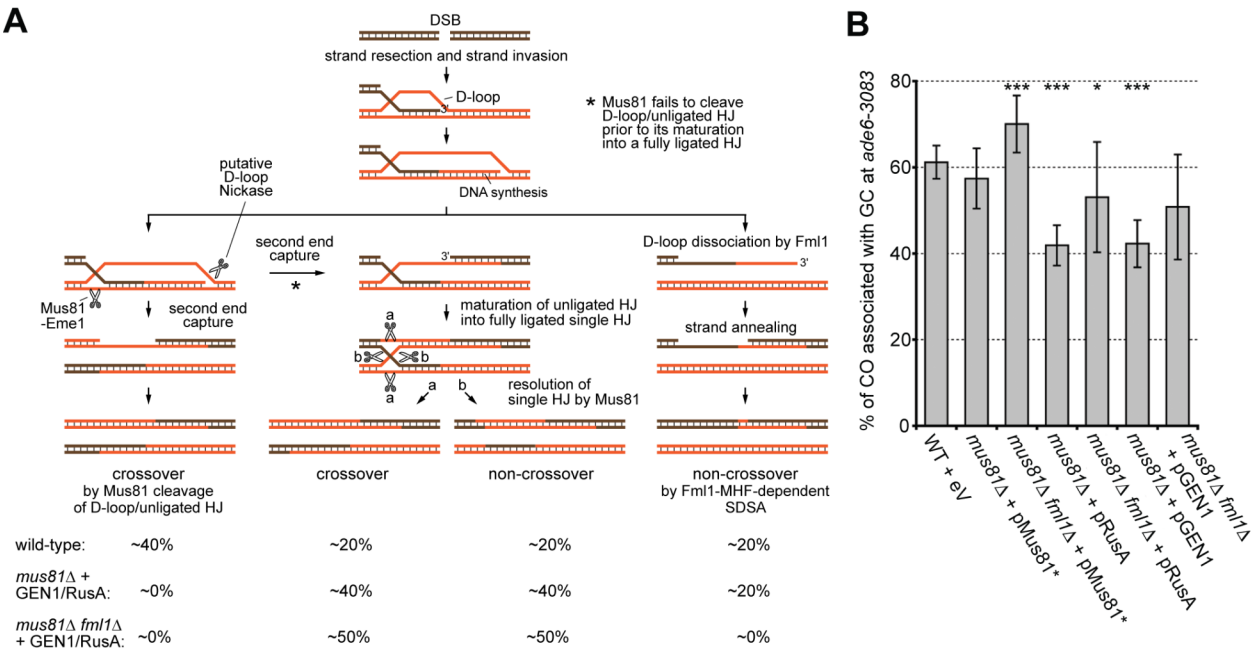

Fig. 4. Meiotic interhomologue recombination pathways in *S. pombe*. (**A**) The respective contribution of recombination pathways to the CO/NCO outcome and the changes observed when a pathway is deactivated. This model accounts for the fact that in a *mus81*Δ strain, only single HJs are observed to accumulate (*10*), but therefore it needs to invoke a D loop nickase activity (*18*). (**B**) Frequency of CO associated with GC events at *ade6-3083* from wild-type, *mus81*Δ, and *mus81*Δ *fml1*Δ crosses expressing Mus81-Eme1, RusA or GEN1$^{(1-527)}$. Statistical significance in comparison with wild type is shown as **P* <0.1, ***P* <0.05, and ****P* <0.01 (table S9) (*18*).

Originally published on www.sciencemag.org/cgi/content/full/336/6088/1585/DC1

Supplementary Material for

The Fission Yeast FANCM Ortholog Directs Non-Crossover Recombination During Meiosis

Alexander Lorenz, Fekret Osman, Weili Sun, Saikat Nandi, Roland Steinacher,
Matthew C. Whitby*

*To whom correspondence should be addessed. E-mail: matthew.whitby@bioch.ox.ac.uk

Published in final edited form as:
Science. 2012 June 22; 336 (6088):1585-1588. doi: 10.1126/science.1220111

This PDF file includes:

METHODS

Yeast strains and plasmid construction. *Schizosaccharomyces pombe* strains used for this study are listed in Table S10. Yeast cells were cultured in YES broth and on YES plates, unless they contained plasmids, in which case the cells were grown in PMG broth and on PMG (or EMMG in the case of fig. S5) agar plates containing the required supplements (concentration ~250 µg/ml). Sporulation of crosses were performed on ME agar, expect for crosses with strains containing plasmids, which were done on SPAS agar supplemented with the required amino acids (concentration ~50 µg/ml). Determination of spore viability by random spore analysis and the meiotic recombination assay have been previously described in detail (*12, 17, 21, 22*).

The *sfr1* gene was deleted in strain ALP729 using *natMX4* as the selectable marker, by cloning up- and downstream flanking sequences of *sfr1* into pAG25 (*23*). This construct removes the complete open reading frame except for 6 nucleotides at the 5' end. The resulting strain was verified by PCR and genotoxin testing. For *dmc1* the *ura4*$^{+}$ gene in an already existing *dmc1*Δ::*ura4*$^{+}$ strain was targeted with a construct carrying the *natMX4* marker from pAG25, from this transformation clonNAT-resistant Ura^{-} colonies were selected.

All plasmids used in this study have been verified by sequencing. Plasmids pREP41 (*24*), pFml1^{+} (pMW848, pREP41-Fml1) (*6*), pFml1^{++} (pALo64, pREP1-Fml1; the *fml1* open reading frame was excised from pMW848 as a SalI-SmaI fragment and cloned into pREP1), pFml1-K99R (pALo70, pREP1-Fml1-K99R; introducing an A296G point mutation into *fml1* using QuikChange XL site-directed mutagenesis, Agilent Technologies, CA), pFml1-D196N (pALo71, pREP1-Fml1-D196N; introducing a G586A point mutation into *fml1* using QuikChange XL site-directed mutagenesis), pFbh1^{+} (pMW637, pREP41-Fbh1) (*25*), pSrs2^{+} (pIJ9, pREP41-Srs2) (*25*), pRqh1^{+} (pMW563, pREP41-Rqh1) (*18*), pFml2^{+} (pMW849, pREP41-Fml2; the *fml2* open reading frame was amplified from genomic DNA and cloned as NdeI-BamHI fragment into pREP41), pRusA (pMW437, pREP1-NLS-RusA-GFP) (*26*), pMus81* (pMW592, pREP41-2myc6his-Mus81–Pk-Eme1) (*17*), pGEN1^{+} (pALo52, pREP41-GEN1$^{(1\text{-}527)}$) (*18*), and pGEN1^{++} (pALo61, pREP1-GEN1$^{(1\text{-}527)}$; the GEN1$^{(1\text{-}527)}$ sequence was excised from pALo52 as a BamHI-NcoI fragment and cloned into pREP1) were transformed into fission yeast strains FO808, FO1260, FO1267, MCW1221, MCW1237, MCW1238, MCW3202/ALP733, MCW3514/ALP802, MCW4994/ALP1170, and MCW5169/ALP1267, and the resulting strains tested for spore viability and in the meiotic recombination assay. Note that in our experiments with GEN1 we use an active truncated form (GEN1$^{1\text{-}527}$) because it expresses well in *S. pombe* and has been characterized extensively in vitro (*18, 27, 28*).

Meiotic time courses, microscopy and gel electrophoresis of crossover DNA products. The protocol for azygotic and *pat1-114* diploid meiotic time courses has been described in detail (*29*). Samples of each time course were fixed in 70% ethanol, stained with Hoechst 33342 and their meiotic progression was checked by assessing the relative numbers of uni-nucleate, horsetail, and multi-nucleate cells in 60 minute intervals. Spreading of nuclei and subsequent processing was performed as described previously (*29*). For immunostaining rabbit α-Rec10 (*30*) and mouse α-c-Myc (Sigma-Aldrich Company Ltd., Dorset, UK) antibodies were used. All analysis was performed using an Olympus BX50 epifluorescence microscope equipped with the appropriate filter sets to detect red, green, and blue fluorescence (Chroma Technology Corp., VT). Black-and-white images were taken with a CoolSNAP HQ^2 CCD camera (Photometrics, AZ) steered by MetaMorph software (v7.7.3.0, Molecular Devices Inc., CA). Images were pseudo-coloured and overlayed using Adobe Photosop CS5 (v12.0, Adobe Systems Inc., CA). Physical analysis of crossover products at *mbs1* was performed as outlined previously (*31*).

D loop binding and unwinding assays. We have been unable to purify full-length Fml1 and therefore for biochemical assays active C-terminally truncated forms of Fml1, Fml1-K99R, and Fml1-D196N were purified and tested for D loop binding and unwinding as described (*6*). Binding reactions (20 µl) contained 0.5 nM labeled D loop in binding buffer (50 mM Tris-HCl, pH 8.0, 1 mM DTT, 100 µg/ml BSA, 6% glycerol). Reactions were started by addition of protein and incubated for 15 minutes on ice before resolving bound and unbound DNA on a 4% native polyacrylamide gel in low ionic strength buffer (6.7 mM Tris-HCl, pH 8.0, 3.3 mM sodium acetate, 2 mM EDTA). Unwinding reactions (20 µl) contained 0.5 nM labeled D loop in binding buffer plus 2.5 mM $MgCl_2$ and 5 mM ATP. Reactions were started by addition of protein and incubated for 30 minutes at 37 °C before being stopped by adding 5 µl of stop mix (2.5% SDS, 200 mM EDTA, 10 mg/ml proteinase K) and further incubation at 37 °C for 15 minutes to deproteinize the mixture. Products were analyzed by electrophoresis through a 10% native polyacrylamide gel in 1 x TBE buffer. Gels were dried on 3 MM Whatman paper and analyzed with a Fuji FLA3000 PhosphorImager (Fujifilm Corp., Japan).

Statistics. Statistical analysis for the recombination data was performed in Excel (Microsoft Office), in G*Power 3.1.3 (Department of Psychology, Heinrich-Heine-University Düsseldorf, Germany) and on http://www.socr.ucla.edu/SOCR.html (University of California, Los Angeles). First each data set was tested for normal distribution using a Shapiro-

Wilk test (http://dittami.gmxhome.de/shapiro/), rejecting the null hypothesis (H_0; 'data fits a normal distribution') at an α-level of $p<0.05$. Several data sets did not conform to a normal distribution and therefore all comparisons were done using a two-tailed, two independent sample Wilcoxon rank-sum test (a.k.a. Mann-Whitney U test). This test is non-parametric and does not depend on data sets being normally distributed. The *P* values of tests against the appropriate wild-type controls are presented in Supplementary Tables S1, S2, S3, S4, and S9. The *P* values of the Fisher's exact test in Table S7 are given for a comparison with the *mus81*Δ cross and were calculated at a statistical power of $1-\beta > 0.95$. H_0 ('data sets being similar') was rejected at an α-level $P<0.1$. In Figs. 1B-D, 2C, 3A, and 4B $P<0.01$ is indicated by three asterisks, $P>0.01<0.05$ by two, and $P>0.05<0.1$ by one.

SUPPLEMENT

Table S1. Frequency of gene conversion and crossing over in the *ura4*$^+$*-aim2 – ade6 – his3*$^+$*-aim* interval. The values are the means from *n* independent crosses and the values in brackets are the standard deviations. The number of Ade$^+$ recombinants tested is indicated, as is the total number of viable spores analyzed for crossing over between *ura4*$^+$*-aim2* and *his3*$^+$*-aim*. *ade6-M26* is a known hot spot for recombination and therefore acts predominantly as a recipient of genetic information, this and the order of markers explains the disparity between P1/R1 and P2/R2 classes. CentiMorgan (cM) are calculated from the accumulated data of the independent crosses, not from the mean values, using the mapping function of Haldane. *P* values are calculated by a two-tailed Mann-Whitney U test against the data from the wild-type cross (MCW1196 × MCW1195).

Cross					% ade$^+$					Crossovers (CO)	
strain	genotype	*n*	Frequency of ade$^+$ in %	ade$^+$ tested	ura$^-$his$^+$ (P1)	ura$^+$his$^-$ (P2)	ura$^-$his$^-$ (R1)	ura$^+$his$^+$ (R2)	tested	Frequency of CO in %	cM
MCW1196 × MCW1195	wild type	20	0.304 (0.108)	3,501	6.58 (2.57)	31.64 (5.92)	57.28 (6.11)	4.5 (3.01)	5,562	12.702 (3.94)	14.69
MCW1832 × MCW1785	*fbh1*Δ[§]	18	0.785[a,§] (0.263)	1,392	11.63[b] (5.45)	32.0[b] (5.2)	49.07[b] (7.74)	7.3[b] (3.4)	1,703	16.988[c] (7.152)	21.72[§]
FO1360 × FO1368	*rqh1*Δ	15	0.024[d] (0.006)	718	7.72[e] (2.61)	27.33[e] (6.22)	59.43[e] (5.56)	5.52[e] (3.31)	2,044	3.09[f] (1.039)	3.13
FO1346 × FO1354	*srs2*Δ	10	0.258[g] (0.048)	1,867	5.06[h] (1.29)	32.39[h] (3.44)	60.08[h] (4.63)	2.47[h] (1.08)	1,437	8.387[i] (1.449)	9.22
MCW3187 × MCW3185	*fml1*Δ	7	0.235[j] (0.093)	1,142	10.79[k] (4.03)	19.23[k] (3.88)	67.56[k] (6.32)	2.42[k] (1.42)	2,663	14.895[l] (2.829)	18.08
MCW3189 × MCW3186	*fml2*Δ	8	0.136[m] (0.029)	582	7.34[n] (2.64)	29.45[n] (3.15)	61.04[n] (3.36)	2.17[n] (1.42)	3,734	11.031[o] (1.517)	11.85
MCW3183 × MCW3182	*fml1*Δ *fml2*Δ[†]	8	0.217[p] (0.087)	1,219	11.88[q] (3.37)	18.56[q] (5.99)	67.06[q] (8.69)	2.5[q] (2.32)	3,426	14.366[r] (3.516)	16.81

[a] $P = 1.885 \times 10^{-6}$, highly significant; [b] $P = 0.027$, significant at an α-level of 0.05; [c] $P = 0.019$, significant at an α-level of 0.05.
[d] $P = 5.733 \times 10^{-7}$, highly significant; [e] $P = 0.177$, not significant; [f] $P = 5.733 \times 10^{-7}$, highly significant.
[g] $P = 0.312$, not significant; [h] $P = 0.725$, not significant; [i] $P = 2.073 \times 10^{-3}$, highly significant.
[j] $P = 0.143$, not significant; [k] $P = 9.311 \times 10^{-3}$, highly significant; [l] $P = 0.121$, not significant.
[m] $P = 1.367 \times 10^{-4}$, highly significant; [n] $P = 0.286$, not significant; [o] $P = 0.416$, not significant.
[p] $P = 0.067$, significant at an α-level of 0.1; [q] $P = 3.747 \times 10^{-3}$, highly significant; [r] $P = 0.242$, not significant.
[§] data from Ref. (*2*), overall the GC and the CO frequencies are increased in *fbh1*Δ compared to wild type, something that was not as pronounced, especially for the COs, in our previous data set (*2*). This increase in GC and CO could be caused by either more DSBs or by changes in the interhomolog bias (similar to what has been suggested for RTEL-1 (*20*)). Previously, *fbh1*Δ has been shown to have poor spore viability, therefore we cannot discount the possibility that it has an effect on the CO/NCO decision during meiosis (*2*).
[†] Fml2 and Fml1 are paralogs, and therefore have the potential to be functionally redundant with each other. We included the *fml1*Δ *fml2*Δ double mutant in our analysis to test this possibility.

Table S2. Frequency of gene conversion and crossing over in the *ura4*$^+$*-aim2 – ade6 – his3*$^+$*-aim* interval. The values are the means from *n* independent crosses and the values in brackets are the standard deviations. The number of Ade$^+$ recombinants tested is indicated, as is the total number of viable spores analyzed for crossing over between *ura4*$^+$*-aim2* and *his3*$^+$*-aim*. *ade6-3083* is a known hot spot for recombination and therefore acts predominantly as a recipient of genetic information, this and the order of markers explains the disparity between P1/R1 and P2/R2 classes. CentiMorgan (cM) are calculated from the accumulated data of the independent crosses, not from the mean values, using the mapping function of Haldane. *P* values are calculated by a two-tailed Mann-Whitney U test against the data from the wild-type cross (ALP733 × ALP731).

Cross					% ade$^+$					Crossovers (CO)	
strain	genotype	*n*	Frequency of ade$^+$ in %	ade$^+$ tested	ura$^-$his$^+$ (P1)	ura$^+$his$^-$ (P2)	ura$^-$his$^-$ (R1)	ura$^+$his$^+$ (R2)	tested	Frequency of CO in %	cM
ALP733 × ALP731	wild type	21	1.371 (0.515)	4,014	4.3 (3.14)	35.34 (6.92)	58.18 (5.71)	2.18 (1.47)	3,265	13.424 (5.33)	15.83
ALP1133 × MCW4718	*fml1*Δ	12	1.171[a] (0.329)	2,069	5.17[b] (1.62)	22.69[b] (2.96)	70.6[b] (2.53)	1.55[b] (0.57)	2,091	13.157[c] (2.545)	15.52
ALP1255 × ALP1231	*fml1-K99R*	11	1.681[d] (0.201)	3,200	6.45[e] (1.3)	20.99[e] (3.03)	70.57[e] (2.91)	1.99[e] (0.64)	2,123	18.108[f] (5.076)	21.86
ALP1277 × ALP1274	*mhf1*Δ	10	0.891[g] (0.248)	1,326	4.22[h] (1.83)	28.31[h] (4.91)	65.79[h] (5.61)	1.68[h] (0.84)	1,552	13.838[i] (4.171)	15.78
ALP1278 × ALP1276	*mhf2*Δ	12	0.984[j] (0.204)	1,513	5.22[k] (2.41)	25.8[k] (4.81)	65.86[k] (6.37)	3.12[k] (1.47)	1,689	15.266[l] (5.532)	20.14
ALP800 × ALP782	*sfr1*Δ*-2*	10	0.11[m] (0.026)	2,429	3.66[n] (1.6)	43.94[n] (2.93)	49.43[n] (2.51)	2.96[n] (1.88)	2,486	2.664[o] (1.838)	2.73
ALP1134 × MCW4719	*fml1*Δ *sfr1*Δ*-2*	12	0.096[p] (0.021)	2,313	4.0[q] (1.39)	25.84[q] (3.51)	68.17[q] (3.78)	1.99[q] (0.85)	2,484	3.396[r] (2.046)	3.63
ALP802 × ALP822	*mus81*Δ[§]	10	0.227[s] (0.085)	46	2.0[t] (6.32)	94.89[t] (11.1)	0.0[t]	3.11[t] (9.85)	1,115	1.932[u] (1.399)	2.06
ALP824 × ALP823	*mus81*Δ *sfr1*Δ*-2*	19	0.029[v] (0.009)	745	1.04[w] (1.56)	92.56[w] (5.88)	5.61[w] (5.4)	0.8[w] (1.55)	3,178	3.179[x] (2.596)	2.85
ALP1365 × ALP1364 or MCW4720	*fml1*Δ *mus81*Δ *sfr1*Δ*-2*	11	<0.00005[y]	n. a.					1,509	1.269[z] (1.056)	1.34
MCW6074 × MCW6075	*mhf1*Δ *mhf2*Δ	8	0.792[A] (0.184)	1,269	4.18[B] (3.76)	25.13[B] (4.08)	64.72[B] (10.04)	5.97[B] (5.4)	1,6199	19.46[C] (4.669)	25.36
ALP1318 × ALP1317	*fml1*Δ *mhf1*Δ *mhf2*Δ	6	0.914[D] (0.08)	1,107	3.61[E] (1.87)	27.29[E] (2.88)	58.41[E] (4.74)	10.69[E] (0.74)	1,308	21.272[F] (7.999)	26.36
ALP1545 ×	*dmc1*Δ*-12*	6	0.509[G]	1,045	3.09[H]	34.29[H]	60.68[H]	1.94[H]	1,164	6.821[I]	7.29

ALP1544			(0.058)		(1.8)	(4.7)	(4.21)	(0.94)		(2.423)	
ALP1092 × ALP1091	*slx1*Δ	12	0.712[K] (0.288)	2,975	5.25[L] (2.11)	32.03[L] (3.41)	59.16[L] (3.79)	3.56[L] (0.94)	4,837	14.787[M] (5.087)	20.08
ALP1104 × ALP1103	*rad16*Δ	12	1.205[N] (0.245)	3,545	3.94[O] (1.19)	34.39[O] (2.37)	59.35[O] (2.93)	2.33[O] (1.18)	3,118	15.856[P] (2.988)	19.29

[a] $P = 0.41$, not significant; [b] $P = 2.897 \times 10^{-6}$, highly significant; [c] $P = 1.0$, not significant.
[d] $P = 0.159$, not significant; [e] $P = 5.549 \times 10^{-6}$, highly significant; [f] $P = 0.041$, significant at an α-level of 0.05.
[g] $P = 0.025$, significant at an α-level of 0.05; [h] $P = 0.007$, highly significant; [i] $P = 0.899$, not significant.
[j] $P = 0.061$, significant at an α-level of 0.1; [k] $P = 2.449 \times 10^{-4}$, highly significant; [l] $P = 0.575$, not significant.
[m] $P = 9.12 \times 10^{-6}$, highly significant; [n] $P = 8.427 \times 10^{-4}$, highly significant; [o] $P = 9.12 \times 10^{-6}$, highly significant.
[p] $P = 2.412 \times 10^{-6}$, highly significant; [q] $P = 3.884 \times 10^{-5}$, highly significant; [r] $P = 7.093 \times 10^{-6}$, highly significant.
[s] $P = 9.12 \times 10^{-6}$, highly significant; [t] $P = 9.12 \times 10^{-6}$, highly significant; [u] $P = 9.12 \times 10^{-6}$, highly significant; [s, t, u] data is corrected for skewed random assortment of unlinked markers, as decribed previously (*12*).
[v] $P = 6.54 \times 10^{-8}$, highly significant; [w] $P = 6.54 \times 10^{-8}$, highly significant; [x] $P = 2.861 \times 10^{-7}$, highly significant; [x] data is corrected for strongly distorted crossing over frequencies.
[y] This is an estimate, there were no ade$^+$ colonies among 32,276 plated spores; [z] $P = 4.592 \times 10^{-6}$, highly significant.
[A] $P = 5.021 \times 10^{-3}$, highly significant; [B] $P = 1.28 \times 10^{-3}$, highly significant; [C] $P = 0.017$, significant at an α-level of 0.05.
[D] $P = 0.162$, not significant; [E] $P = 4.267 \times 10^{-3}$, highly significant; [F] $P = 0.031$, significant at an α-level of 0.05.
[G] $P = 2.386 \times 10^{-4}$, highly significant; [H] $P = 0.382$, not significant; [I] $P = 7.301 \times 10^{-3}$, highly significant. Although *dmc1*Δ shows moderate, but highly significant reductions in gene conversion at *ade6* and crossing over between *ura4*$^+$*-aim2 – his3*$^+$*-aim*, it does not influence the CO/NCO-ratio associated with a gene conversion event. This indicates that Dmc1 is involved in choosing the homologous chromosome over the sister chromatid as a template (as previously discussed (*32, 33*)), but does not impinge on the CO/NCO-decision once an extended D loop is formed.
[K] $P = 7.567 \times 10^{-4}$, highly significant; [L] $P = 0.262$, not significant; [M] $P = 0.389$, not significant.
[N] $P = 0.389$, not significant; [O] $P = 0.765$, not significant; [P] $P = 0.217$, not significant.
[§] data from Ref. (*18*)

Table S3. Frequency of gene conversion and crossing over in the *ura4*$^+$*-aim2 – ade6 – his3*$^+$*-aim* interval. The values are the means from *n* independent crosses and the values in brackets are the standard deviations. The number of Ade$^+$ recombinants tested is indicated, as is the total number of viable spores analyzed for crossing over between *ura4*$^+$*-aim2* and *his3*$^+$*-aim*. *ade6-M375* is a known cold spot for meiotic DSB formation. Nevertheless recombination induced at this site causes a disparity between P1/R1 and P2/R2 classes, since *ade6-M375* is the recipient of genetic information. CentiMorgan (cM) are calculated from the accumulated data of the independent crosses, not from the mean values, using the mapping function of Haldane. *P* values are calculated by a two-tailed Mann-Whitney U test against the data from the wild-type cross (ALP1541 × ALP731).

Cross					**% ade$^+$**					**Crossovers (CO)**	
strain	**genotype**	***n***	**Frequency of ade$^+$ in %**	**ade$^+$ tested**	**ura$^-$his$^+$ (P1)**	**ura$^+$his$^-$ (P2)**	**ura$^-$his$^-$ (R1)**	**ura$^+$his$^+$ (R2)**	**tested**	**Frequency of CO in %**	**cM**
ALP1541 × ALP731	wild type	6	0.0278 (0.0036)	1,053	6.39 (2.46)	34.44 (2.66)	56.74 (4.45)	2.42 (0.62)	1,083	10.075 (3.539)	11.70
MCW1832 × MCW1785	*fml1*Δ	6	0.0474[a] (0.0105)	1,166	7.5[b] (0.87)	24.62[b] (1.39)	65.32[b] (2.16)	2.57[b] (0.95)	1,155	14.988[c] (3.558)	17.68

[a] $P = 0.025$, significant at an α-level of 0.05; [b] $P = 0.004$, highly significant; [c] $P = 0.055$, significant at an α-level of 0.1.

Table S4. Frequency of crossing over in the *his1-102 – leu2-120 – lys7-2* interval. The values are the means from *n* independent crosses, the values in brackets are the standard deviations. The total number of viable spores analyzed for crossing over between *his1* and *leu2*, *leu2* and *lys7*, as well as *his1* and *lys7*. Since *leu2* is located inbetween *his1* and *lys7*, the segregation pattern of *leu2-120* in these crosses was used to determine the frequency of double crossovers in the *his1 – lys7* interval. CentiMorgan (cM) are calculated from the accumulated data of the independent crosses, not from the mean values, using the mapping function of Haldane. *P* values are calculated by a two-tailed Mann-Whitney U test against the data from the wild-type cross (ALP996 × ALP1002).

Cross				**Crossovers (CO)**					
strain	**genotype**	***n***	**tested**	***his1-102 leu2-120***		***leu2-120 lys7-2***		***his1-102 (leu2-120) lys7-2***	
ALP996 × ALP1002	wild type	5	723	16.393 % (1.614)	19.96 cM	10.868 % (1.409)	12.15 cM	25.899 % (1.469)	36.42 cM
ALP1014 × ALP1017	*fml1*Δ	5	825	21.244 %[a] (1.733)	27.39 cM	13.689 %[b] (3.544)	15.51 cM	32.133 %[c] (3.841)	50.08 cM

[a] $P = 0.008$, highly significant; [b] $P = 0.151$, not significant; [c] $P = 0.032$, significant at an α-level of 0.05.

Table S5. Spore viability

strain	cross	spore viability in % of plated spores, numbers in brackets are spores plated/experiment [a]										Mean ± s.d. [a]
WT	ALP714 × ALP688	61.41 (894)	73.85 (891)	82.4 (915)	75.41 (915)	59.68 (930)	102.7 (888)	80.6 (897)	80.35 (921)	91.32 (1,371)	61.5 (891)	76.92 ± 13.8 (9,513)
*fml1*Δ	ALP989 × ALP990	89.44 (900)	72.05 (891)	69.16 (921)	76.46 (909)	59.42 (924)	60.82 (906)	64.09 (891)	68.2 (915)	63.29 (888)	102.96 (879)	72.59 ± 13.84 (9,024)
fml1-K99R	ALP1255 × ALP1231	68.14 (948)	55.79 (864)	56.37 (1,020)	50.61 (903)	68.31 (975)	57.19 (918)	65.42 (1,044)	65.73 (966)	59.16 (999)	57.85 (987)	60.46 ± 6.04 (9,624)
*sfr1*Δ *-2*	ALP797 × ALP775	54.75 (1,527)	57.84 (861)	55.95 (924)	47.15 (2,859)	41.49 (1,239)	48.32 (1,341)	41.19 (1,272)	38.51 (1,332)	53.14 (1,449)	43.6 (1,383)	48.19 ± 6.92 (14,187)
*fml1*Δ *sfr1*Δ*-2*	ALP1135 × ALP1136	36.95 (1,356)	47.32 (1,380)	41.59 (1,380)	33.58 (1,212)	53.22 (1,287)	40.55 (1,344)	54.82 (1,182)	33.57 (1,248)	51.65 (1,179)	43.5 (1,269)	43.68 ± 7.86 (12,837)
*mus81*Δ	ALP812 × ALP813	3.47 (132,600)	4.88 (133,200)	2.61 (32,400)	2.99 (60,900)	1.08 (45,000)	0.82 (24,000)	1.25 (25,200)	0.65 (27,000)	0.33 (27,000)	0.39 (54,000)	1.85 ± 1.55 (561,300)
*mus81*Δ *sfr1*Δ*-2*	ALP820 × ALP814	38.60 (2,184)	28.27 (4,563)	27.34 (5,508)	20.77 (3,510)	21.34 (3,276)	46.04 (2,541)	32.55 (2,160)	38.29 (2,220)	26.07 (2,562)	29.7 (2,566)	30.9 ± 8.06 (31,090)
*fml1*Δ *mus81*Δ *sfr1*Δ*-2*	ALP1167 × ALP1168	5.35 (24,000)	4.45 (36,000)	1.77 (37,050)	1.2 (37,800)	1.4 (43,500)	2.96 (37,950)	0.58 (36,000)	1.42 (36,000)	2.69 (38,250)	0.71 (39,000)	2.25 ± 1.6 (365,550)
WT + eV	MCW1221 × FO808 + pREP41	64.65 (843)	83.5 (921)	61.18 (912)	58.62 (911)	59.66 (870)	79.67 (915)	68.9 (894)	69.06 (918)	66.44 (885)	61.71 (888)	67.34 ± 8.38 (8,957)
WT + pFml1^{+}	ALP733 × FO1267 + pREP41-Fml1	75.74 (672)	70.54 (662)	85.76 (667)	71.72 (693)	79.56 (680)	74.16 (685)	78.81 (703)	71.12 (696)	88.24 (689)	69.66 (745)	76.53 ± 6.48 (6,892)
WT + pFml1^{++}	ALP733 × FO1267 + pREP1-Fml1	80.79 (807)	51.34 (859)	62.22 (847)	61.03 (816)	68.96 (931)	72.7 (923)	83.47 (847)	56.81 (808)	73.02 (882)	52.29 (853)	66.26 ± 11.32 (8,573)
WT + pFml1-K99R	ALP733 × FO1267 + pREP1-Fml1-K99R	67.27 (828)	48.85 (827)	56.28 (844)	69.96 (839)	64.48 (853)	48.22 (869)	65.33 (721)	52.94 (918)	59.31 (870)	91.6 (762)	62.42 ± 12.77 (8,331)
WT + pFml1-D196N	ALP733 × FO1267 + pREP1-Fml1-D196N	74.57 (936)	64.72 (958)	62.2 (926)	57.42 (923)	63.19 (910)	55.3 (944)	62.73 (907)	60.31 (955)	52.69 (947)	71.49 (891)	62.46 ± 6.76 (9,297)
*mus81*Δ + eV	MCW1238 × MCW1237 + pREP41	0.8 (19,800)	1.2 (16,200)	1.08 (16,380)	0.33 (28,800)	0.84 (14,700)	3.98 (33,000)	3.85 (8,100)	3.65 (8,400)	4.43 (9,450)	3.16 (8,100)	2.33 ± 1.61 (162,930)
*mus81*Δ + pFml1^{+}	ALP802 × FO1260 + pREP41-Fml1	21.36 (9,800)	22.93 (5,425)	18.64 (4,200)	15.19 (5,775)	19.32 (10,150)	17.2 (5,075)	23.33 (4,050)	23.65 (6,650)	24.8 (4,025)	12.54 (6,125)	19.9 ± 4.04 (61,275)
*mus81*Δ + pFml1^{++}	ALP802 × FO1260 + pREP1-Fml1	18.33 (6,300)	18.18 (6,150)	27.5 (5,040)	25.83 (5,280)	19.89 (6,240)	17.1 (6,450)	15.74 (6,450)	16.53 (5,070)	16.27 (5,550)	16.45 (6,000)	19.18 ± 4.15 (58,530)
*mus81*Δ + pFml1-K99R	ALP802 × FO1260 + pREP1-Fml1-K99R	0.02 (45,000)	0.05 (42,000)	0.06 (44,100)	0.05 (45,000)	0.13 (48,000)	0.13 (43,500)	0.12 (45,000)	0.09 (48,300)	0.09 (43,200)	0.03 (46,800)	0.08 ± 0.04 (450,900)
*mus81*Δ + pFml1-D196N	ALP802 × FO1260 + pREP1-Fml1-D196N	0.15 (39,000)	0.06 (63,000)	0.13 (93,000)	0.11 (93,000)	0.06 (66,000)	0.05 (84,000)	0.07 (72,000)	0.11 (99,000)	0.07 (93,000)	0.07 (114,000)	0.09 ± 0.03 (816,000)
*mus81*Δ + pFbh1^{+}	ALP802 × FO1260 + pREP41-Fbh1	1.55 (5,925)	1.45 (7,950)	0.97 (7,500)	1.54 (7,200)	1.12 (7,800)	1.33 (9,825)					1.33 ± 0.24 (46,200)
*mus81*Δ + pSrs2^{+}	ALP802 × FO1260 + pREP41-Srs2	1.28 (9,450)	3.19 (6,525)	2.09 (5,700)	2.07 (6,750)	1.71 (7,650)	1.84 (6,150)					2.03 ± 0.64 (42,225)
*mus81*Δ + pRqh1^{+}	ALP802 × FO1260 + pREP41-Rqh1	0.35 (6,000)	0.6 (4,500)	0.67 (5,100)	0.35 (8,400)	0.74 (9,150)	0.91 (5,700)					0.6 ± 0.22 (38,850)
*mus81*Δ + pFml2^{+}	ALP802 × FO1260 + pREP41-Fml2	1.33 (6,000)	2.2 (4,050)	1.5 (5,850)	1.98 (5,850)	0.78 (6,000)	1.26 (9,600)					1.51 ± 0.51 (37,350)
*rec12*Δ*-171*	ALP1428 × ALP1429	34.47 (1,938)	38.93 (1,662)	33.88 (2,010)	26.76 (2,238)	20.84 (1,761)	28.83 (1,644)					30.62 ± 6.45 (11,253)
*rec12*Δ*-171 mus81*Δ *sfr1*Δ*-2*	ALP1472 × ALP1473	25.96	27.47	29.66	38.98	23.19	30.45					29.28 ± 5.42

		(1,668)	(1,809)	(1,740)	(1,719)	(1,647)	(1,698)					(10,281)
rec12Δ-171 fml1Δ mus81Δ	ALP1470 × ALP1471	12.52 (2,268)	13.47 (2,376)	12.49 (2,409)	12.26 (2,520)	10.08 (2,580)						12.16 ± 1.26 (12,153)
rec12Δ-171 fml1Δ mus81Δ sfr1Δ-2	ALP1474 × ALP1475	15.83 (1,800)	14.32 (1,836)	15.06 (1,800)	15.34 (1,695)	13.29 (1,851)	19.94 (1,710)					15.63 ± 2.29 (10,692)
*fml1Δ mus81Δ + pMus81**	ALP1170 × ALP1267 + pREP41-Mus81-Eme1	20.53 (2,250)	37.1 (2,418)	8.47 (2,610)	32.26 (2,430)	15.87 (2,439)						22.85 ± 11.75 (12,147)
fml1Δ mus81Δ + pRusA	ALP1170 × ALP1267 + pREP1-rusA	13.82 (6,000)	6.83 (6,240)	7.19 (5,940)	7.91 (6,120)	19.37 (6,300)	16.33 (6,105)					11.91 ± 5.35 (36,705)
fml1Δ mus81Δ + pGEN1^{++}	ALP1170 × ALP1267 + pREP1-GEN1$^{(1-527)}$	0.76 (5,400)	0.79 (7,200)	0.92 (5,100)	0.96 (5,400)	1.11 (4,950)	1.26 (4,200)					0.97 ± 0.19 (32,250)
rqh1Δ	ALP783 × ALP784	26.17 (1,028)	34.98 (972)	28.01 (1,389)	36.76 (1,314)	30.49 (1,197)	30.69 (1,554)	44.17 (1,560)	21.89 (1,599)	31.03 (2,340)	29.98 (2,295)	31.42 ± 6.12 (15,248)
srs2Δ	MCW1017 × MCW1016 *FO1346 × FO1354	78.0 (600)	77.0 (600)	80.0 (600)	70.0* (750)	72.0* (750)						75.4 ± 4.22 (3,300)
fml2Δ	ALP1576 × ALP1575	74.52 (777)	53.0 (832)	49.7 (843)	79.89 (756)	79.78 (811)	90.27 (771)					71.2 ± 16.23 (4,790)
dmc1Δ-12	ALP1545 × ALP1544	43.96 (1,035)	72.66 (1,006)	67.94 (814)	51.08 (1,016)	82.03 (1,085)	70.92 (1,049)					64.77 ± 14.34 (6,005)
slx1Δ	ALP1083 × ALP1084	85.47 (888)	86.84 (1,011)	88.06 (1,131)	61.92 (927)	41.08 (852)	68.33 (903)	62.98 (867)	62.6 (885)	67.02 (849)	74.48 (921)	69.88 ± 14.48 (9,234)
rad16Δ	ALP1117 × ALP1118	60.47 (1,032)	48.9 (912)	62.31 (918)	48.91 (963)	59.94 (996)	58.38 (978)	66.04 (963)	74.45 (1,002)	42.49 (786)	41.67 (936)	56.36 ± 10.59 (9,486)
slx1Δ mus81Δ sfr1Δ-2	ALP1089 × ALP1090	29.88 (2,952)	29.41 (2,928)	30.17 (3,096)	38.22 (2,640)	28.51 (3,048)	39.5 (3,000)	30.4 (2,970)	34.68 (2,970)	29.35 (2,964)	26.72 (2,934)	31.68 ± 4.29 (29,502)
rad16Δ mus81Δ sfr1Δ-2	ALP1143 × ALP1144	23.35 (2,814)	29.51 (6,228)	28.85 (2,880)	22.0 (3,222)	30.13 (3,030)	34.91 (3,165)	23.43 (2,808)	27.71 (6,243)	31.79 (3,108)	33.05 (3,150)	28.47 ± 4.36 (36,648)

[a] numbers in brackets represent total number of plated spores (n).
eV stands for empty vector.

Table S6. Percentage of asci formed in a mating population. Strains with different mating types were mixed together, plated onto solid sporulation media and incubated at +25°C before being inspected after 2 and 3 days under a standard light microscope, except for the *mus81Δ fml1Δ* double mutant (ALP1050 × ALP1051), which was followed for 7 days.

Cross		*n*		
strain	**genotype**	**total cells tested**	**% Asci**	**Standard Deviation**
ALP714 × ALP688	wild type	1,541	42.93	1.75
ALP989 × ALP990	*fml1Δ*	1,167	34.27	1.76
ALP812 × ALP813	*mus81Δ*	1,419	26.69	1.51
ALP797 × ALP775	*sfr1Δ*	1,038	36.21	6.21
ALP820 × ALP814	*mus81Δ sfr1Δ*	1,125	19.90	5.57
ALP1050 × ALP1051	*fml1Δ mus81Δ*	3,929	0.81	0.45
ALP1167 × ALP1168	*fml1Δ mus81Δ sfr1Δ*	1,383	10.91	4.19

Table S7. Distribution of DNA masses in wild-type and mutant asci with or without over-expression of wild-type and mutant Fml1. Asci were classified into five categories: (I) 4 regularly distributed DNA masses, (II) 1 DNA mass (total segregation failure), (III) more than 1 but less than 4 DNA masses (partial segregation failure), (IV) 4 irregularly distributed DNA masses (mis-segregation of chromosomes), and (V) more than 4 DNA masses (DNA fragmentation). Percentage of asci in each category is given. Strains with different mating types were mixed together, plated onto solid sporulation media and incubated at +25°C for several days. Cells were stained with Hoechst33342 and evaluated under an epifluorescence microscope. *P* values are calculated by a one-tailed Fisher's exact test against the data from the *mus81*Δ cross (ALP812 × ALP813).

Strains crossed	genotype	n	I	II	III	IV	V
ALP714 × ALP688	*wild type*	107	99.065	0.0	0.0	0.0	0.935
ALP989 × ALP990	*fml1*Δ	117	88.034	0.0	5.983	5.983	0.0
ALP797 × ALP775	*sfr1*Δ	127	29.134	0.787	20.472	47.244	2.362
ALP812 × ALP813	*mus81*Δ	113	0.0	38.938	47.788	9.735	3.54
ALP820 × ALP814	*mus81*Δ *sfr1*Δ	90	6.667	2.222[a]	23.333	50.0	17.778
ALP1050 × ALP1051	*fml1*Δ *mus81*Δ	101	0.0	46.535[b]	43.564	8.911	0.99
ALP1167 × ALP1168	*fml1*Δ *mus81*Δ *sfr1*Δ	133	0.0	40.602[c]	42.105	10.526	6.767
ALP802 × FO1260 + pFml1^{+}	*mus81*Δ + pREP41-Fml1	114	0.0	22.807[d]	42.982	24.561	9.649
ALP802 × FO1260 + pFml1-K99R	*mus81*Δ + pREP1-Fml1-K99R	113	0.0	48.673[e]	32.743	14.159	4.425
ALP802 × FO1260 + pFml1-D196N	*mus81*Δ + pREP1-Fml1-D196N	134	0.0	46.269[f]	35.075	14.925	3.731

[a] $P = 4.089 \times 10^{-12}$, highly significant
[b] $P = 0.008$, highly significant
[c] $P = 0.565$, not significant
[d] $P = 1.278 \times 10^{-4}$, highly significant
[e] $P = 3.119 \times 10^{-6}$, highly significant
[f] $P = 0.006$, highly significant

Table S8. Mus81 foci in Rec10-positive nuclei of wild-type and *sfr1*Δ-*2* strains (for details on staging of Rec10-stained linear elements see fig. S4).

	dots	threads	networks	bundles
wild type (ALP1524)				
% of Mus81-positive nuclei	20.0	28.6	100.0	80.0
Average number of Mus81 foci/nucleus	0.4	0.67	19.6	16.4
Maximum number of Mus81 foci	4	5	49	47
n	20	21	28	15
sfr1*Δ-*2 (ALP1540)				
% of Mus81-positive nuclei	20.0	25.0	68.2	53.3
Average number of Mus81 foci/nucleus	0.35	0.45	5.27	4.53
Maximum number of Mus81 foci	2	4	34	27
n	20	20	22	15

Table S9. Frequency of gene conversion and crossing over in the *ura4*$^+$*-aim2 – ade6 – his3*$^+$*-aim* interval. The values are the means from *n* independent crosses and the values in brackets are the standard deviations. The number of Ade$^+$ recombinants tested is indicated, as is the total number of viable spores analyzed for crossing over between *ura4*$^+$*-aim2* and *his3*$^+$*-aim*. *ade6-3083* is a known hot spot for recombination and therefore acts predominantly as a recipient of genetic information, this and the order of markers explains the disparity between P1/R1 and P2/R2 classes. CentiMorgan (cM) are calculated from the accumulated data of the independent crosses, not from the mean values, using the mapping function of Haldane. *P* values are calculated by a two-tailed Mann-Whitney U test against the data from the wild-type cross (ALP733 × FO1267 + pREP41).

Cross					% ade$^+$					Crossovers (CO)	
strain	genotype	*n*	Frequency of ade$^+$ in %	ade$^+$ tested	ura$^-$his$^+$ (P1)	ura$^+$his$^-$ (P2)	ura$^-$his$^-$ (R1)	ura$^+$his$^+$ (R2)	tested	Frequency of CO in %	cM
ALP733 × FO1267 + pREP41	wild type + empty vector[§]	12	0.803 (0.098)	2,247	2.79 (1.17)	36.02 (4.11)	58.29 (3.86)	2.89 (2.09)	2,374	13.628 (4.951)	15.82
ALP733 × FO1267 + pFml1$^+$	wild type + pREP41-Fml1	12	0.969[a] (0.081)	2,359	2.05[b] (1.05)	43.47[b] (3.94)	51.57[b] (3.16)	2.91[b] (1.42)	2,470	10.505[c] (2.424)	11.87
ALP733 × FO1267 + pFml1^{++}	wild type + pREP1-Fml1	11	1.055[d] (0.119)	2,314	3.53[e] (1.59)	45.64[e] (3.72)	46.57[e] (3.89)	4.26[e] (1.39)	2,324	13.889[f] (5.265)	16.11
ALP733 × FO1267 + pFml1-K99R	wild type + pREP1-Fml1-K99R	11	0.897[g] (0.173)	1,876	5.55[h] (2.0)	26.72[h] (2.76)	65.43[h] (2.22)	2.29[h] (0.83)	1,987	17.262[i] (2.953)	21.25
ALP733 × FO1267 + pFml1-D196N	wild type + pREP1-Fml1-D196N	12	1.077[j] (0.19)	2,310	4.96[k] (1.59)	25.48[k] (3.98)	67.7[k] (3.49)	1.86[k] (1.08)	2,545	15.631[l] (2.601)	18.76
ALP802 × FO1260 + pFml1$^+$	*mus81*Δ + pREP41-Fml1	12	0.52[m] (0.102)	1,117	1.7[n] (1.56)	93.38[n] (4.5)	0.8[n] (1.56)	4.12[n] (3.72)	2,404	3.086[o] (1.465)	3.4
ALP802 × FO1260 + pMus81*	*mus81*Δ + pREP41-Mus81-Eme1[§]	10	0.98[p] (0.216)	1,445	3.26[q] (1.14)	39.33[q] (6.9)	53.57[q] (7.22)	3.84[q] (2.24)	1,504	12.986[r] (3.381)	15.91
ALP1170 × ALP1267 + pMus81*	*fml1*Δ *mus81*Δ + pREP41-Mus81-Eme1	7	1.492[s] (0.495)	532	7.67[t] (3.0)	22.28[t] (4.16)	66.97[t] (5.55)	3.08[t] (1.78)	366	19.454[u] (8.064)	26.83
ALP802 × FO1260 + pRusA	*mus81*Δ + pREP1-rusA[§]	13	0.836[v] (0.295)	2,047	8.78[w] (4.12)	49.36[w] (7.21)	29.9[w] (7.24)	11.96[w] (6.92)	2,088	11.892[x] (4.308)	12.75
ALP1170 × ALP1267	*fml1*Δ *mus81*Δ + pREP1-rusA	12	0.759[y] (0.2)	500	11.04[z] (5.67)	35.88[z] (14.28)	43.71[z] (12.17)	9.37[z] (5.15)	4,039	15.852[Λ] (6.77)	18.41

+ pRusA											
ALP802 × FO1260 + pGEN1^{+}	*mus81*Δ + pREP41-GEN1$^{(1-527)}$§	12	0.744^{B} (0.137)	2,054	4.15^{C} (1.5)	53.59^{C} (4.72)	36.18^{C} (6.29)	6.08^{C} (2.36)	2,683	10.611^{D} (5.95)	10.73
ALP1170 × ALP1267 + pGEN1^{+}	*fml1*Δ *mus81*Δ + pREP41-GEN1$^{(1-527)}$	4	0.272^{E} (0.065)	32	8.33^{F} (16.67)	42.71^{F} (13.77)	46.18^{F} (12.6)	2.78^{F} (5.56)	485	11.374^{G} (1.204)	13.13
ALP1170 × ALP1267 + pGEN1^{++}	*fml1*Δ *mus81*Δ + pREP1-GEN1$^{(1-527)}$	7	0.515^{H} (0.455)	140	3.25^{J} (4.23)	45.96^{J} (11.11)	44.06^{J} (8.92)	6.73^{J} (6.78)	1,859	17.388^{K} (4.415)	20.61

[a] $P = 9.987 \times 10^{-4}$, highly significant; [b] $P = 5.32 \times 10^{-4}$, highly significant; [c] $P = 0.149$, not significant.
[d] $P = 2.218 \times 10^{-4}$, highly significant; [e] $P = 4.865 \times 10^{-5}$, highly significant; [f] $P = 1.0$, not significant.
[g] $P = 0.074$, significant at an α-level of 0.1; [h] $P = 4.513 \times 10^{-4}$, highly significant; [i] $P = 0.176$, not significant.
[j] $P = 5.32 \times 10^{-4}$, highly significant; [k] $P = 2.755 \times 10^{-4}$, highly significant; [l] $P = 0.644$, not significant.
[m] $P = 4.146 \times 10^{-5}$, highly significant; [n] $P = 3.226 \times 10^{-5}$, highly significant; [o] $P = 4.146 \times 10^{-5}$, highly significant.
[p] $P = 0.075$, significant at an α-level of 0.1; [q] $P = 0.187$, not significant; [r] $P = 0.553$, not significant.
[s] $P = 0.007$, highly significant; [t] $P = 0.009$, highly significant; [u] $P = 0.176$, not significant.
[v] $P = 0.301$, not significant; [w] $P = 2.209 \times 10^{-5}$, highly significant; [x] $P = 0.301$, not significant.
[y] $P = 0.119$, not significant; [z] $P = 0.057$, significant at an α-level of 0.1 (tested against *mus81*Δ + pREP1-rusA: $P = 2.0 \times 10^{-3}$, highly significant); [A] $P = 0.686$, not significant.
[B] $P = 0.141$, not significant; [C] $P = 3.226 \times 10^{-5}$, highly significant; [D] $P = 0.248$, not significant.
[E] $P = 0.004$, highly significant; [F] $P = 0.332$, not significant; [G] $P = 0.396$, not significant.
[H] $P = 0.011$, significant at an α-level of 0.05; [J] $P = 0.099$, significant at an α-level of 0.1; [K] $P = 0.128$, not significant.
§ data from Ref. (*18*)

Table S10. Strain list

Strain	*Relevant genotype*	Origin
MCW1196	*h^{+N} ade6-469 his3^{+}-aim his3-D1 leu1-32 ura4-D18*	Ref. (*12*)
MCW1195	*h^{-} ade6-M26 ura4^{+}-aim2 arg3-D4 his3-D1 ura4-D18*	Ref. (*12*)
MCW1832	*h^{+N} fbh1Δ::kanMX6 ade6-M26 ura4^{+}-aim2 arg3-D4 his3-D1 leu1-32 ura4-D18*	Ref. (*2*)
MCW1785	*h^{-} fbh1Δ::kanMX6 ade6-469 his3^{+}-aim arg3-D4 his3-D1 leu1-32 ura4-D18*	Ref. (*2*)
FO1360	*h^{+N} rqh1Δ::kanMX6 ade6-469 his3^{+}-aim his3-D1 leu1-32 ura4-D18*	this study
FO1368	*h^{-} rqh1Δ::kanMX6 ade6-M26 ura4^{+}-aim2 arg3-D4 his3-D1 ura4-D18*	this study
FO1346	*h^{+N} srs2Δ::kanMX6 ade6-M26 ura4^{+}-aim2 arg3-D4 his3-D1 ura4-D18*	this study
FO1354	*h^{-smt0} srs2Δ::kanMX6 ade6-469 his3^{+}-aim his3-D1 leu1-32 ura4-D18*	this study
MCW3187	*h^{+N} fml1Δ::natMX4 ade6-469 his3^{+}-aim his3-D1 leu1-32 ura4-D18*	this study
MCW3185	*h^{-} fml1Δ::natMX4 ade6-M26 ura4^{+}-aim2 arg3-D4 his3-D1 ura4-D18*	this study
MCW3189	*h^{+N} fml2Δ::kanMX6 ade6-469 his3^{+}-aim his3-D1 leu1-32 ura4-D18*	this study
MCW3186	*h^{-} fml2Δ::kanMX6 ade6-M26 ura4^{+}-aim2 arg3-D4 his3-D1 ura4-D18*	this study
MCW3183	*h^{+N} fml1Δ::natMX4 fml2Δ::kanMX6 ade6-469 his3^{+}-aim his3-D1 leu1-32 ura4-D18*	this study
MCW3182	*h^{-} fml1Δ::natMX4 fml2Δ::kanMX6 ade6-M26 ura4^{+}-aim2 arg3-D4 his3-D1 ura4-D18*	this study
MCW3202/ALP733	*h^{+S} ade6-3083 ura4^{+}-aim2 his3-D1 leu1-32 ura4-D18*	Ref. (*18*)
MCW3200/ALP731	*h^{-smt0} ade6-469 his3^{+}-aim arg3-D4 his3-D1 ura4-D18*	Ref. (*18*)
MCW4881/ALP1133	*h^{+S} fml1Δ::hphMX4 ade6-3083 ura4^{+}-aim2 his3-D1 leu1-32 ura4-D18*	this study
MCW4718/FO2608	*h^{-smt0} fml1Δ::hphMX4 ade6-469 his3^{+}-aim arg3-D4 his3-D1 ura4-D18*	this study
MCW5136/ALP1255	*h^{+S} fml1-K99R::natMX4 ade6-3083 ura4^{+}-aim2 his3-D1 leu1-32 ura4-D18*	this study
MCW5093/ALP1231	*h^{-smt0} fml1-K99R::natMX4 ade6-469 his3^{+}-aim arg3-D4 his3-D1 ura4-D18*	this study
MCW5185/ALP1277	*h^{+S} mhf1Δ::kanMX6 ade6-3083 ura4^{+}-aim2 his3-D1 leu1-32 ura4-D18*	this study
MCW5182/ALP1274	*h^{-smt0} mhf1Δ::kanMX6 ade6-469 his3^{+}-aim arg3-D4 his3-D1 ura4-D18*	this study
MCW5186/ALP1278	*h^{+S} mhf2Δ::natMX4 ade6-3083 ura4^{+}-aim2 his3-D1 leu1-32 ura4-D18*	this study
MCW5184/ALP1276	*h^{-smt0} mhf2Δ::natMX4 ade6-469 his3^{+}-aim arg3-D4 his3-D1 ura4-D18*	this study
MCW4473/ALP996	*h^{+N} lys7-2*	this study
MCW4507/ALP1002	*h^{-} his1-102 leu2-120*	this study
MCW4543/ALP1014	*h^{+N} fml1Δ::natMX4 lys7-2*	this study
MCW4546/ALP1017	*h^{-} fml1Δ::natMX4 his1-102 leu2-120*	this study
ALP714	*h^{+S}*	this study
ALP688	*h^{-smt0}*	this study
MCW4475/ALP989	*h^{+S} fml1Δ::natMX4*	this study
MCW4476/ALP990	*h^{-smt0} fml1Δ::natMX4*	this study
MCW3497/ALP797	*h^{+S} sfr1Δ-2::natMX4*	this study
MCW3355/ALP775	*h^{-smt0} sfr1Δ-2::natMX4*	this study
MCW4885/ALP1135	*h^{+S} fml1Δ::hphMX4 sfr1Δ-2::natMX4*	this study
MCW4886/ALP1136	*h^{-smt0} fml1Δ::hphMX4 sfr1Δ-2::natMX4*	this study
MCW3542/ALP812	*h^{+S} mus81Δ::kanMX6*	this study
MCW3543/ALP813	*h^{-smt0} mus81Δ::kanMX6*	this study
MCW3587/ALP820	*h^{+S} mus81Δ::kanMX6 sfr1Δ-2::natMX4*	this study
MCW3544/ALP814	*h^{-smt0} mus81Δ::kanMX6 sfr1Δ-2::natMX4*	this study
MCW4991/ALP1167	*h^{+S} fml1Δ::hphMX4 mus81Δ::kanMX6 sfr1Δ-2::natMX4*	this study
MCW4992/ALP1168	*h^{-smt0} fml1Δ::hphMX4 mus81Δ::kanMX6 sfr1Δ-2::natMX4*	this study
MCW3500/ALP800	*h^{+S} sfr1Δ-2::natMX4 ade6-3083 ura4^{+}-aim2 his3-D1 leu1-32 ura4-D18*	this study
MCW3386/ALP782	*h^{-smt0} sfr1Δ-2::natMX4 ade6-469 his3^{+}-aim arg3-D4 his3-D1 ura4-D18*	this study
MCW4882/ALP1134	*h^{+S} fml1Δ::hphMX4 sfr1Δ-2::natMX4 ade6-3083 ura4^{+}-aim2 his3-D1 leu1-32 ura4-D18*	this study

MCW4719/FO2609	*h^{-smt0} fml1Δ::hphMX4 sfr1Δ-2::natMX4 ade6-469 his3^{+}-aim arg3-D4 his3-D1 ura4-D18*	this study
MCW3514/ALP802	*h^{+S} mus81Δ::kanMX6 ade6-3083 ura4^{+}-aim2 his3-D1 leu1-32 ura4-D18*	Ref. (*18*)
MCW3589/ALP822	*h^{-smt0} mus81Δ::kanMX6 ade6-469 his3^{+}-aim arg3-D4 his3-D1 ura4-D18*	Ref. (*18*)
MCW3591/ALP824	*h^{+S} mus81Δ::kanMX6 sfr1Δ-2::natMX4 ade6-3083 ura4^{+}-aim2 his3-D1 leu1-32 ura4-D18*	this study
MCW3590/ALP823	*h^{-smt0} mus81Δ::kanMX6 sfr1Δ-2::natMX4 ade6-469 his3^{+}-aim arg3-D4 his3-D1 ura4-D18*	this study
MCW5330/ALP1365	*h^{+S} fml1Δ::hphMX4 mus81Δ::kanMX6 sfr1Δ-2::natMX4 ade6-3083 ura4^{+}-aim2 his3-D1 leu1-32 ura4-D18*	this study
MCW5329/ALP1364	*h^{-smt0} fml1Δ::hphMX4 mus81Δ::kanMX6 sfr1Δ-2::natMX4 ade6-469 his3^{+}-aim arg3-D4 his3-D1 ura4-D18*	this study
MCW4720/FO2610	*h^{-smt0} fml1Δ::hphMX4 mus81Δ::kanMX6 sfr1Δ-2::natMX4 ade6-469 his3^{+}-aim arg3-D4 his3-D1 ura4-D18*	this study
MCW4624/ALP1050	*h^{+S} fml1Δ::natMX4 mus81Δ::kanMX6*	this study
MCW4625/ALP1051	*h^{-smt0} fml1Δ::natMX4 mus81Δ::kanMX6*	this study
FO1260	*h^{-} mus81Δ::kanMX6 ade6-469 his3^{+}-aim his3-D1 leu1-32 ura4-D18*	lab strain; Ref. (*18*)
MCW1221	*h^{+N} arg3-D4 his3-D1 leu1-32 ura4-D18*	lab strain; Ref. (*34*)
FO808	*h^{-} arg3-D4 his3-D1 leu1-32 ura4-D18*	lab strain; Ref. (*18*)
FO1267	*h^{-} ade6-469 his3^{+}-aim his3-D1 leu1-32 ura4-D18*	lab strain; Ref. (*18*)
MCW1238/FO909	*h^{+N} mus81Δ::kanMX6 arg3-D4 his3-D1 leu1-32 ura4-D18*	lab strain; Ref. (*18*)
MCW1237/FO908	*h^{-} mus81Δ::kanMX6 arg3-D4 his3-D1 leu1-32 ura4-D18*	lab strain; Ref. (*18*)
MCW5516/ALP1428	*h^{+N} rec12Δ-171::ura4+ ura4-D18*	this study
MCW5517/ALP1429	*h^{-smt0} rec12Δ-171::ura4+ ura4-D18*	this study
MCW5580/ALP1472	*h^{+N} mus81Δ::kanMX6 rec12Δ-171::ura4+ sfr1Δ-2::natMX4 ura4-D18*	this study
MCW5581/ALP1473	*h^{-smt0} mus81Δ::kanMX6 rec12Δ-171::ura4+ sfr1Δ-2::natMX4 ura4-D18*	this study
MCW5578/ALP1470	*h^{+N} fml1Δ::hphMX4 mus81Δ::kanMX6 rec12Δ-171::ura4+ ura4-D18*	this study
MCW5579/ALP1471	*h^{-smt0} fml1Δ::hphMX4 mus81Δ::kanMX6 rec12Δ-171::ura4+ ura4-D18*	this study
MCW5582/ALP1474	*h^{+N} fml1Δ::hphMX4 mus81Δ::kanMX6 rec12Δ-171::ura4+ sfr1Δ-2::natMX4 ura4-D18*	this study
MCW5583/ALP1475	*h^{-smt0} fml1Δ::hphMX4 mus81Δ::kanMX6 rec12Δ-171::ura4+ sfr1Δ-2::natMX4 ura4-D18*	this study
MCW4994/ALP1170	*h^{+S} fml1Δ::hphMX4 mus81Δ::kanMX6 ade6-3083 ura4^{+}-aim2 his3-D1 leu1-32 ura4-D18*	this study
MCW5169/ALP1267	*h^{-smt0} fml1Δ::hphMX4 mus81Δ::kanMX6 ade6-469 his3^{+}-aim his3-D1 leu1-32 ura4-D18*	this study
MCW5788/ALP1541	*h^{+N} ade6-M375 ura4^{+}-aim2 his3-D1 leu1-32 ura4-D18*	this study
MCW5789/ALP1542	*h^{+N} fml1Δ::hphMX4 ade6-M375 ura4^{+}-aim2 his3-D1 leu1-32 ura4-D18*	this study
MCW6074/FO2992	*h^{+N} mhf1Δ::kanMX6 mhf2Δ::natMX4 ade6-469 his3^{+}-aim arg3-D4 his3-D1 ura4-D18*	this study
MCW6075/FO2993	*h^{-} mhf1Δ::kanMX6 mhf2Δ::natMX4 ade6-3083 ura4^{+}-aim2 his3-D1 leu1-32 ura4-D18*	this study
MCW5234/ALP1318	*h^{+S} fml1Δ::hphMX4 mhf1Δ::kanMX6 mhf2Δ::natMX4 ade6-3083 ura4^{+}-aim2 his3-D1 leu1-32 ura4-D18*	this study
MCW5233/ALP1317	*h^{-smt0} fml1Δ::hphMX4 mhf1Δ::kanMX6 mhf2Δ::natMX4 ade6-469 his3^{+}-aim arg3-D4 his3-D1 ura4-D18*	this study
MCW3387/ALP783	*h^{+S} rqh1Δ::kanMX6*	this study
MCW3388/ALP784	*h^{-smt0} rqh1Δ::kanMX6*	this study
MCW1017/FO902	*h^{+N} srs2Δ::ura4^{+}arg3-D4 his3-D1 leu1-32 ura4-D18*	lab strain; Ref. (*34*)
MCW1016/FO901	*h^{-} srs2Δ::ura4^{+}arg3-D4 his3-D1 leu1-32 ura4-D18*	lab strain
MCW6007/ALP1576	*h^{+S} fml2Δ::kanMX6 ade6-3083 ura4^{+}-aim2 his3-D1 leu1-32 ura4-D18*	this study
MCW6006/ALP1575	*h^{-smt0} fml2Δ::kanMX6 ade6-469 his3^{+}-aim arg3-D4 his3-D1 ura4-D18*	this study
MCW5795/ALP1545	*h^{+S} dmc1Δ-12::natMX4 ade6-3083 ura4^{+}-aim2 his3-D1 leu1-32 ura4-D18*	this study
MCW5793/ALP1544	*h^{-smt0} dmc1Δ-12::natMX4 ade6-469 his3^{+}-aim arg3-D4 his3-D1 ura4-D18*	this study
MCW4794/ALP1092	*h^{+S} slx1Δ::kanMX6 ade6-3083 ura4^{+}-aim2 his3-D1 leu1-32 ura4-D18*	this study
MCW4793/ALP1091	*h^{-smt0} slx1Δ::kanMX6 ade6-469 his3^{+}-aim arg3-D4 his3-D1 ura4-D18*	this study
MCW4816/ALP1104	*h^{+S} rad16Δ::kanMX6 ade6-3083 ura4^{+}-aim2 his3-D1 leu1-32 ura4-D18*	this study
MCW4815/ALP1103	*h^{-smt0} rad16Δ::kanMX6 ade6-469 his3^{+}-aim arg3-D4 his3-D1 ura4-D18*	this study
MCW4785/ALP1083	*h^{+S} slx1Δ::kanMX6*	this study
MCW4786/ALP1084	*h^{-smt0} slx1Δ::kanMX6*	this study

MCW4841/ALP1117	*h^{+S} rad16Δ::kanMX6*	this study
MCW4842/ALP1118	*h^{-smt0} rad16Δ::kanMX6*	this study
MCW4791/ALP1089	*h^{+S} mus81Δ::arg3^{+} sfr1Δ-2::natMX4 slx1Δ::kanMX6 arg3-D4*	this study
MCW4792/ALP1090	*h^{-smt0} mus81Δ::arg3^{+} sfr1Δ-2::natMX4 slx1Δ::kanMX6 arg3-D4*	this study
MCW4964/ALP1143	*h^{+S} mus81Δ::arg3^{+} rad16Δ::kanMX6 sfr1Δ-2::natMX4 arg3-D4*	this study
MCW4965/ALP1144	*h^{-smt0} mus81Δ::arg3^{+} rad16Δ::kanMX6 sfr1Δ-2::natMX4 arg3-D4*	this study
MCW5202/ALP1291	*h^{-}/h^{-} mbs1-24/mbs1-25 pat1-114/pat1-114 ade6-M210/ade6-M216 leu1+/leu1-32 ura1+/ura1-61*	this study
MCW5203/ALP1292	*h^{-}/h^{-} mbs1-24/mbs1-25 pat1-114/pat1-114 ade6-M210/ade6-M216 leu1+/leu1-32 ura1+/ura1-61*	this study
MCW5154/ALP1264	*h^{-}/h^{-} fml1Δ::hphMX4/fml1Δ::hphMX4 mbs1-24/mbs1-25 pat1-114/pat1-114 ade6-M210/ade6-M216 leu1+/leu1-32 ura1+/ura1-61*	this study
MCW5155/ALP1265	*h^{-}/h^{-} fml1Δ::hphMX4/fml1Δ::hphMX4 mbs1-24/mbs1-25 pat1-114/pat1-114 ade6-M210/ade6-M216 leu1+/leu1-32 ura1+/ura1-61*	this study
MCW5717/ALP1524	*h^{+N}/h^{-} mus81^{+}::13myc-kanMX6/mus81^{+}::13myc-kanMX6 ade6-M210/ade6-M216*	this study
MCW5787/ALP1540	*h^{+S}/h^{-smt0} sfr1Δ-2::natMX4/sfr1Δ-2::natMX4 mus81^{+}::13myc-kanMX6/mus81^{+} ade6-M210/ade6-M216*	this study
ALP729	*h^{+S} arg3-D4 his3-D1 leu1-32 ura4-D18*	lab strain
MCW2575/ALP500	*h^{+N} dmc1Δ::ura4^{+}arg3-D4 his3-D1 leu1-32 ura4-D18*	lab strain

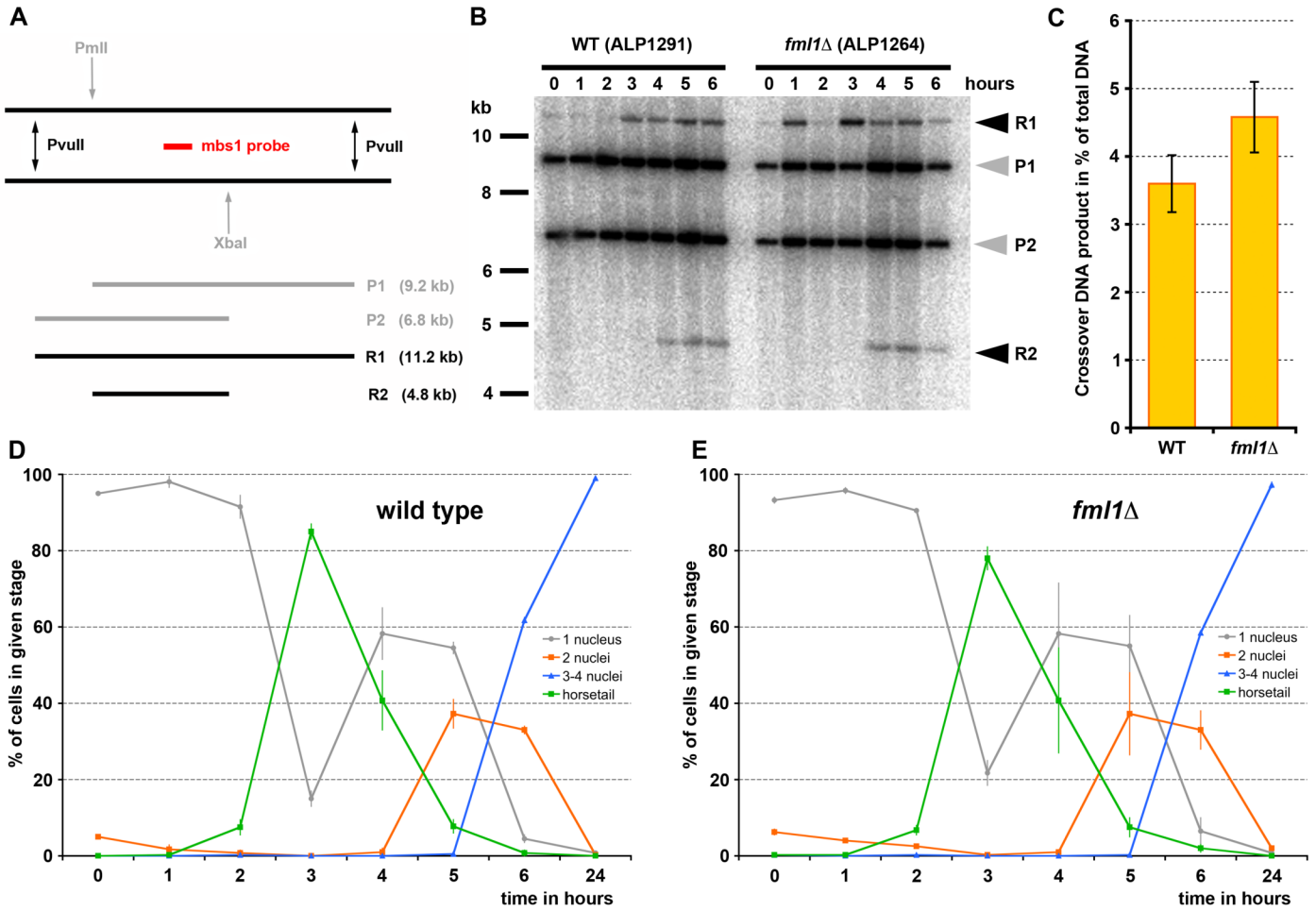

Figure S1. Physical assay for analyzing CO formation during meiosis. (**A**) Schematic of the physical meiotic recombination assay at *mbs1* on chromosome 1. The restriction sites, the position of the probe used at this locus and the sizes of the expected DNA fragments after endonuclease digestion are indicated (*31*). (**B**) Southern Blot showing diploid wild-type and *fml1*Δ meiotic *pat1-114* timecourses with CO products arising by the 4 hour timepoint following meiotic induction. (**C**) Quantification of the CO product at the 6 hour timepoint from Southern blots like in (B). Incomplete digestion results in a band of the same size as R1, therefore the percentage of CO recombination was calculated using 2×R2/total DNA (*33*). (**D**-**E**) Percentage of different meiotic stages evaluated with Hoechst 33342-stained cells in wild-type (ALP1291 and ALP1292) and *fml1*Δ (ALP1264 and ALP1265) timecourses (*29*). (**C**-**E**) Values represent the average of two independent experiments each, error bars indicate the range (experiment 1: WT = 3.18% CO and *fml1*Δ = 4.06% CO; experiment 2: WT = 4.02% CO and *fml1*Δ = 5.10% CO).

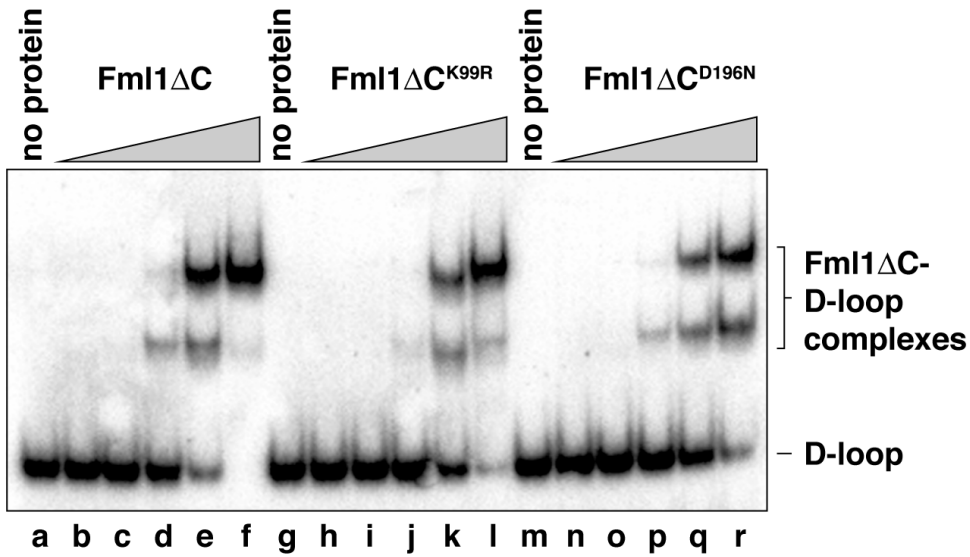

Figure S2. Gel retardation assay showing binding of Fml1ΔC (lanes b – f: 0.05 nM, 0.1 nM, 0.5 nM, 5 nM, and 10 nM), Fml1ΔC-K99R (lane h - l: 0.05 nM, 0.1 nM, 0.5 nM, 5 nM, and 10 nM), and Fml1ΔC-D196N (lanes n – r: 0.05 nM, 0.1 nM, 0.5 nM, 5 nM, and 10 nM) to a synthetic D loop. See Methods for further details.

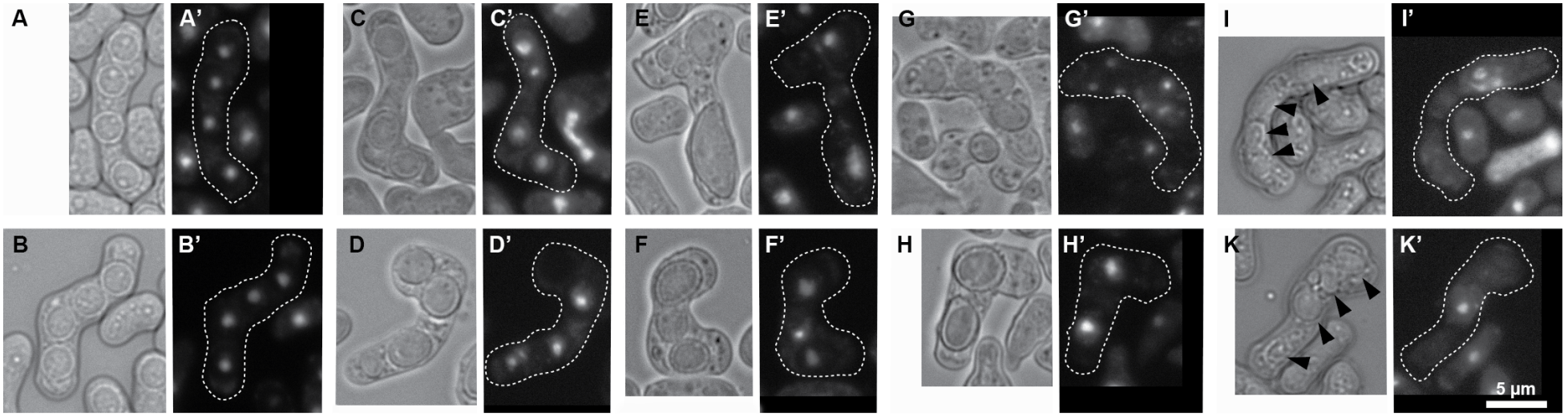

Figure S3. Examples of asci as evaluated in Fig. 2B. **(A-K)** Bright field microscopy images and **(A'-K')** epifluorescence microscopy images of DNA stained with Hoechst 33342. Outlines of the asci are indicated as dashed white lines. **(A, A', B, B')** Asci from a wild-type cross (ALP714 × ALP688) with 4 equally distributed DNA masses. **(C, C')** Asci from a *mus81*Δ *sfr1*Δ-*2* cross (ALP820 × ALP814) with 4 irregularly distributed DNA masses. **(D, D')** Asci from a *sfr1*Δ-*2* cross (ALP797 × ALP775) with 4 irregularly distributed DNA masses. **(E, E')** Asci from a *sfr1*Δ-*2* cross (ALP797 × ALP775) with 2 irregularly distributed DNA masses. **(F, F')** Asci from a *mus81*Δ *sfr1*Δ-*2* cross (ALP820 × ALP814) with 3 irregularly distributed DNA masses. **(G, G')** Asci from a *mus81*Δ *sfr1*Δ-*2* cross (ALP820 × ALP814) with 6 irregularly distributed DNA masses. **(H, H')** Asci from a *sfr1*Δ-*2* cross (ALP797 × ALP775) with 2 regularly distributed DNA masses. **(I, I', K, K')** Asci from a *mus81*Δ cross (ALP812 × ALP813) with a single DNA mass (spores with immature spore walls are indicated by arrowheads). Spore wall formation is normally initiated during meiosis II, this suggests that asci containing less than 4 spores also must have passed meiosis I and the spindle pole body duplication at the onset of meiosis II (reviewed in (*35*)).

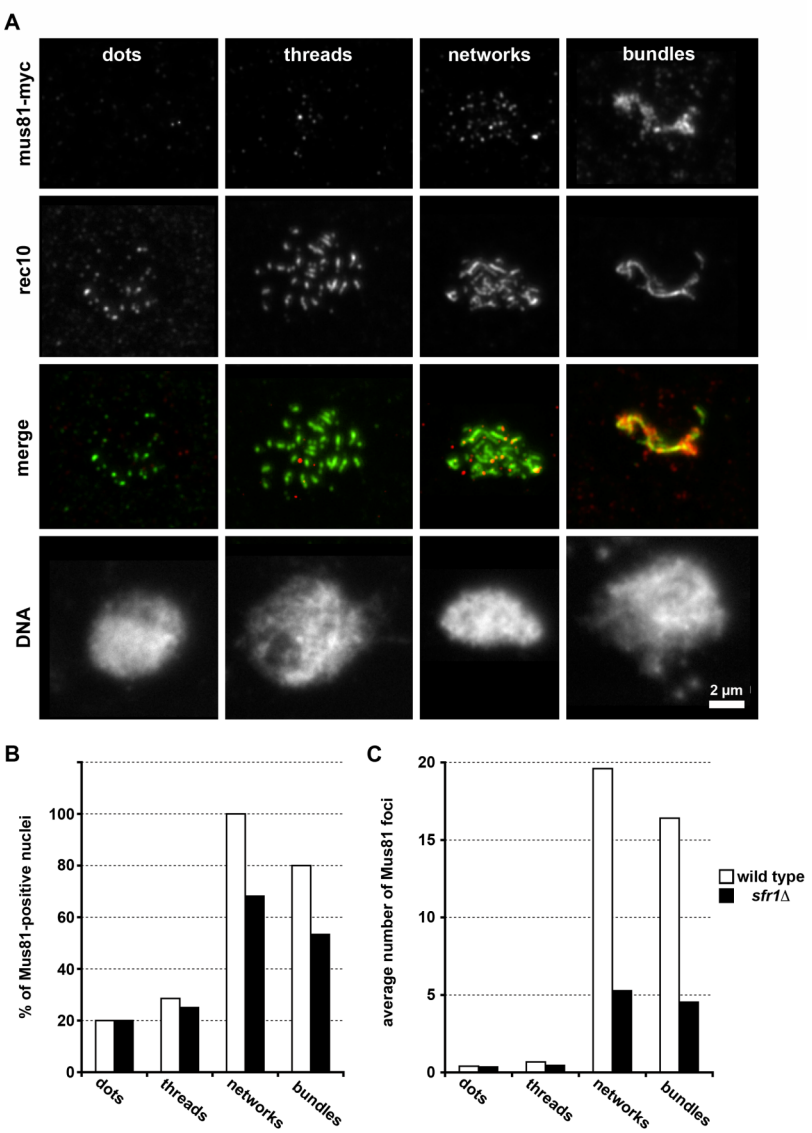

Figure S4. Mus81 focus formation in wild type and *sfr1*Δ-*2*. **(A)** Examples of Mus81 foci in Rec10-positive nuclei of each stage of linear elements from diploid wild type (ALP1524). The row labeled merge shows Rec10 in green and Mus81-13myc in red and the bottom row shows DNA stained with Hoechst 33342. The 4 stages have been shown to accumulate at different time points of a meiotic time course (dots and threads arising early, whereas networks and bundles can be found only in later time points). Rec10 also coincides and colocalizes with different recombination markers, like Rec7 and Rad51 at particular stages (*30, 36*). **(B)** Percentage of Mus81-positive nuclei among meiotic nuclei staged according to their linear element morphology in wild type (ALP1524) and *sfr1*Δ *-2* (ALP1540). **(C)** Average number of Mus81 foci in meiotic nuclei staged according to their linear element morphology in wild type (ALP1524) and *sfr1*Δ *-2* (ALP1540).

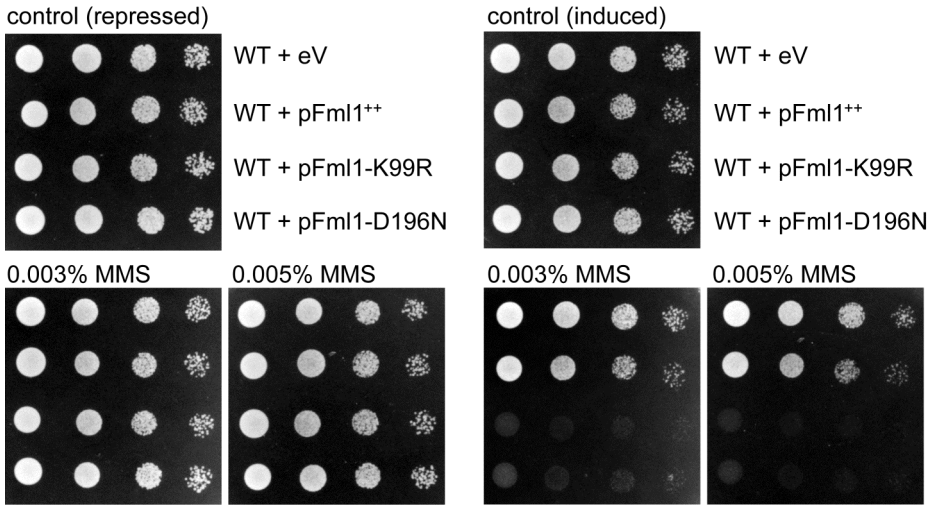

Figure S5. Effect of wild-type and mutant Fml1 over-expression (expressed from the thiamine-repressible *nmt1*-promotor in pREP1) on the sensitivity of a wild-type strain (MCW1221) against the alkalyting agent methyl-methanesulfonate (MMS). pREP1 serves as the empty vector (eV) control. Cells were spotted in a 10-fold dilution series (from 10^5 to 10^2 cells) onto EMMG agar containing thiamine (repressed) and MMS as indicated.

Supplemental References

21. S. A. Sabatinos, S. L. Forsburg, *Methods Enzymol* **470**, 759 (2010).
22. G. R. Smith, *Methods Mol Biol* **557**, 65 (2009).
23. A. L. Goldstein, J. H. McCusker, *Yeast* **15**, 1541 (1999).
24. K. Maundrell, *Gene* **123**, 127 (1993).
25. A. Lorenz, F. Osman, V. Folkyte, S. Sofueva, M. C. Whitby, *Mol Cell Biol* **29**, 4742 (2009).
26. C. L. Doe, J. Dixon, F. Osman, M. C. Whitby, *EMBO J* **19**, 2751 (2000).
27. S. C. Ip *et al.*, *Nature* **456**, 357 (2008).
28. U. Rass *et al.*, *Genes Dev* **24**, 1559 (2010).
29. J. Loidl, A. Lorenz, *Methods Mol Biol* **558**, 15 (2009).
30. A. Lorenz *et al.*, *J Cell Sci* **117**, 3343 (2004).
31. R. W. Hyppa, G. R. Smith, *Methods Mol Biol* **557**, 235 (2009).
32. A. L. Grishchuk, J. Kohli, *Genetics* **165**, 1031 (2003).
33. R. W. Hyppa, G. R. Smith, *Cell* **142**, 243 (2010).
34. F. Osman, J. Dixon, A. R. Barr, M. C. Whitby, *Mol Cell Biol* **25**, 8084 (2005).
35. C. Shimoda, *J Cell Sci* **117**, 389 (2004).
36. A. Lorenz, A. Estreicher, J. Kohli, J. Loidl, *Chromosoma* **115**, 330 (2006).